



Averaging Framework for fNIRS-Based Time Series with Application in Multi-Modal Brain Imaging

Li Zhu

Advisor: Prof. Laleh Najafizadeh

Integrated Systems and NeuroImaging Laboratory
Department of Electrical and Computer Engineering
Rutgers University

05/05/2016

Ph.D. Qualifying Examination



Outline

□ Introduction

- Overview of Neuroimaging Techniques
- Multi-Modal Brain Imaging
- Functional Near-Infrared Spectroscopy
- Experimental Design

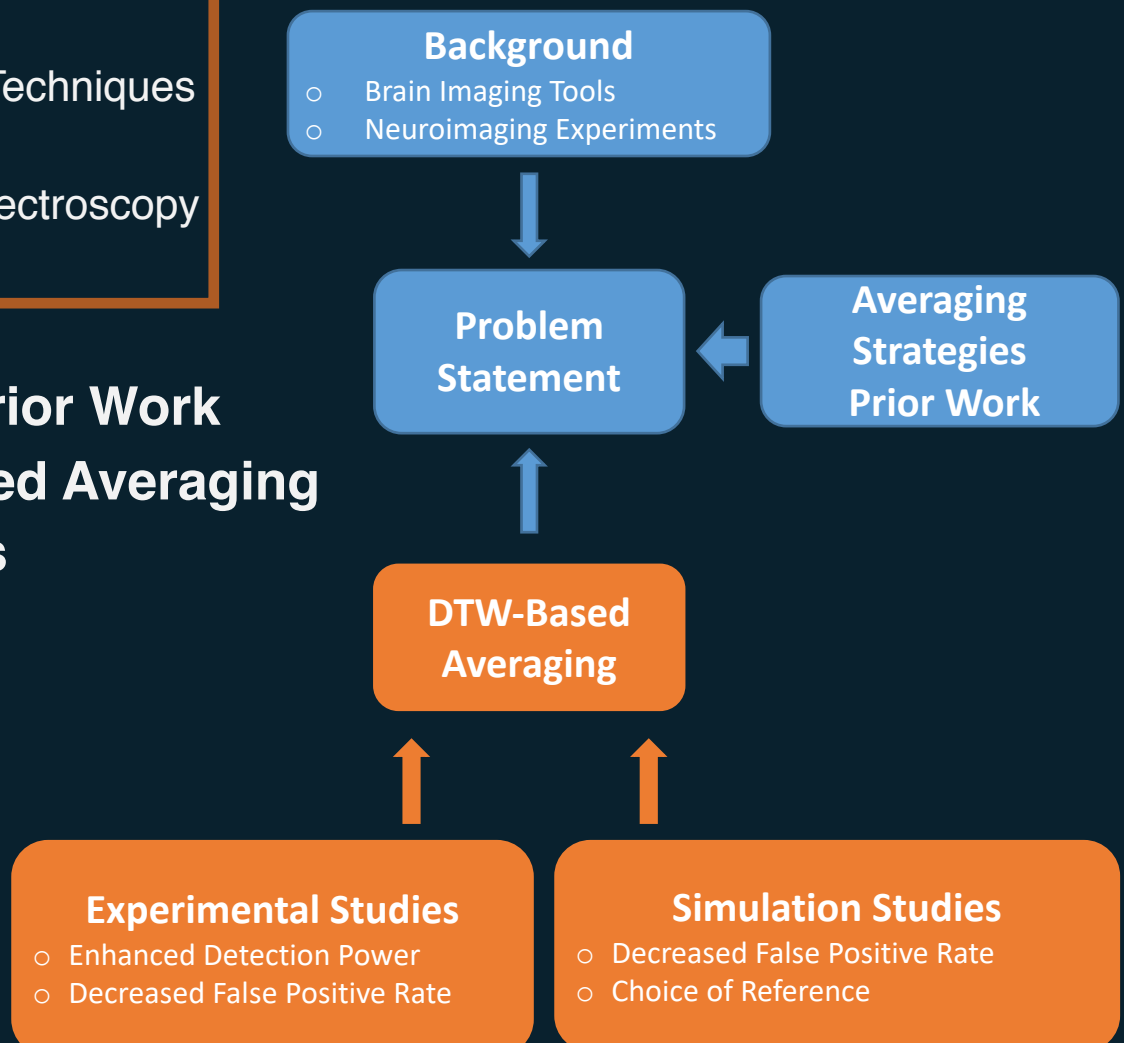
□ Problem Statement

□ Averaging Strategies - Prior Work

□ Framework for DTW-based Averaging

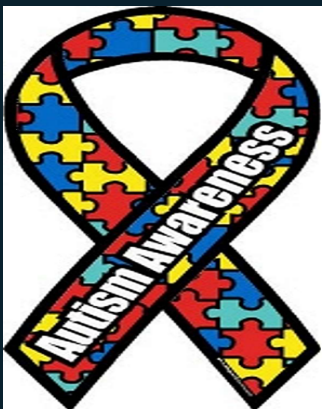
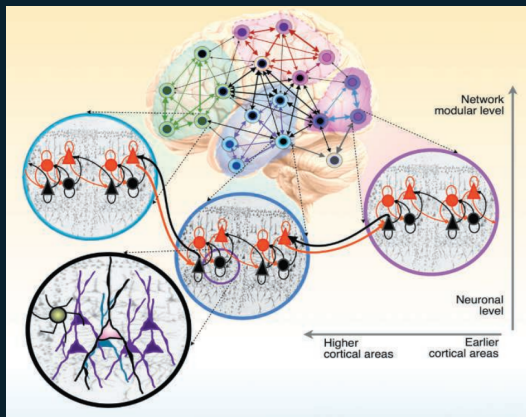
□ Experiments and Results

□ Conclusion



Neuroimaging Techniques

- Human brain: ~ 100 billion neurons, 100,000 Miles of blood vessels
- Diagnosis of brain-related diseases requires variable brain imaging tools
 - Autistic Spectrum Disorders: 1 in 1000 children are diagnosed with Autism
 - 1 in 100 US population are diagnosed with Schizophrenia



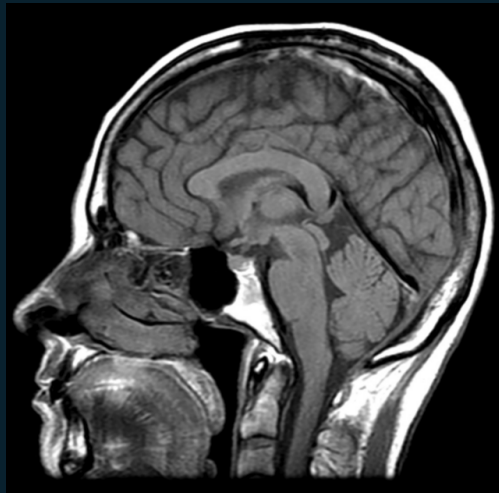
Neuroimaging Techniques



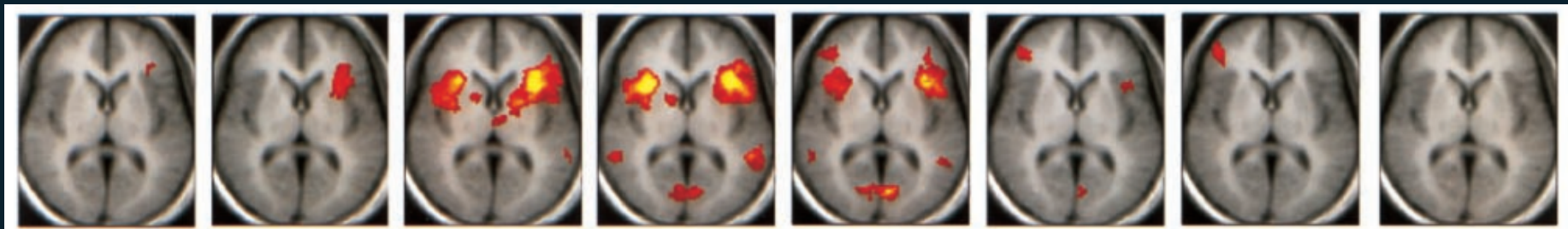
Structural/ Functional

- Structural brain imaging
 - Study the physical structure of the brain.
 - Magnetic Resonance Imaging (MRI)

- Functional brain imaging
 - Study the brain functionality.
 - Functional Magnetic resonance imaging (fMRI)



MRI



fMRI

https://en.wikipedia.org/wiki/Magnetic_resonance_imaging#/media/File:T1t2PD.jpg

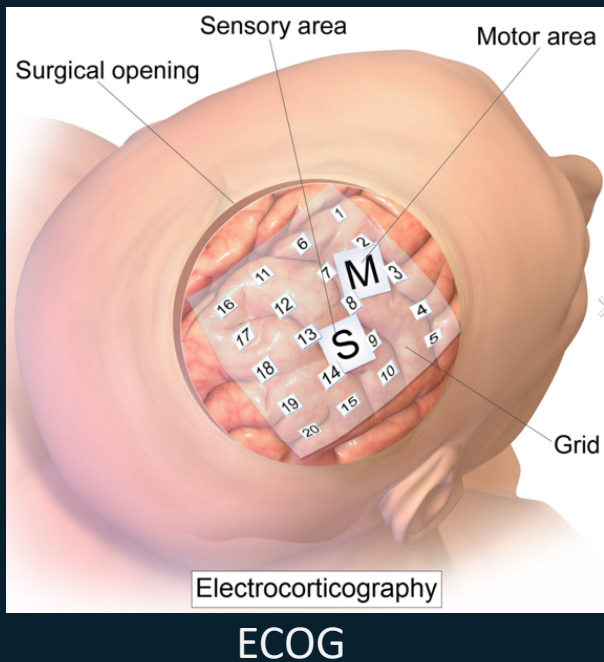
Neuroimaging Techniques



Invasive/ Non-invasive

□ Invasive brain imaging

- Superior spatial resolution while requires open-skull surgery
- Electrocorticography (ECoG)



□ Non-invasive brain imaging

- No open-skull surgery is needed
- Electroencephalography (EEG)
- fMRI
- fNIRS



EEG

Neuroimaging Techniques



Direct/ Indirect measure

- Direct measure of neuronal activity
- Indirect measure of neuronal activity
 - EEG
 - MEG
- fMRI
- fNIRS



EEG



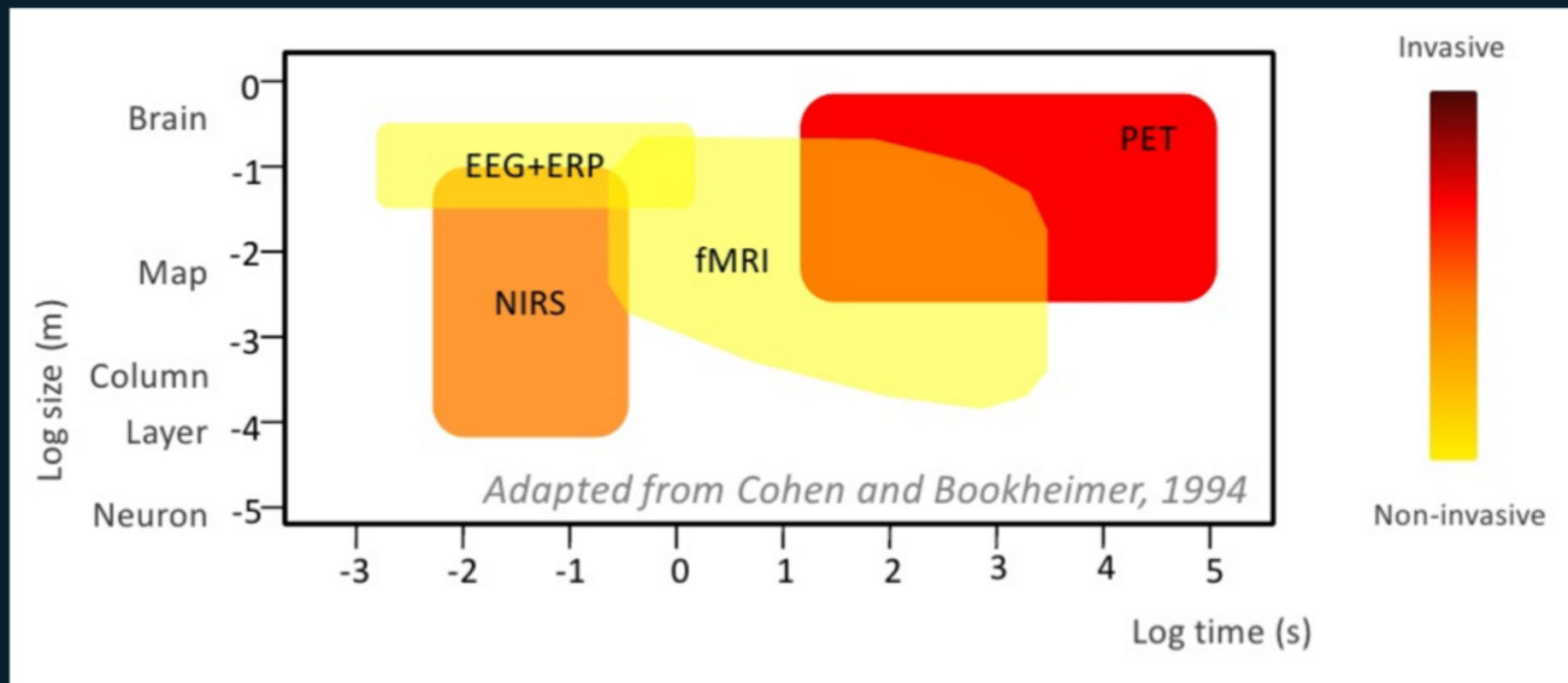
fNIRS

Neuroimaging Techniques



Multi-Modal Brain Imaging

Temporal and Spatial resolution of functional brain imaging tools

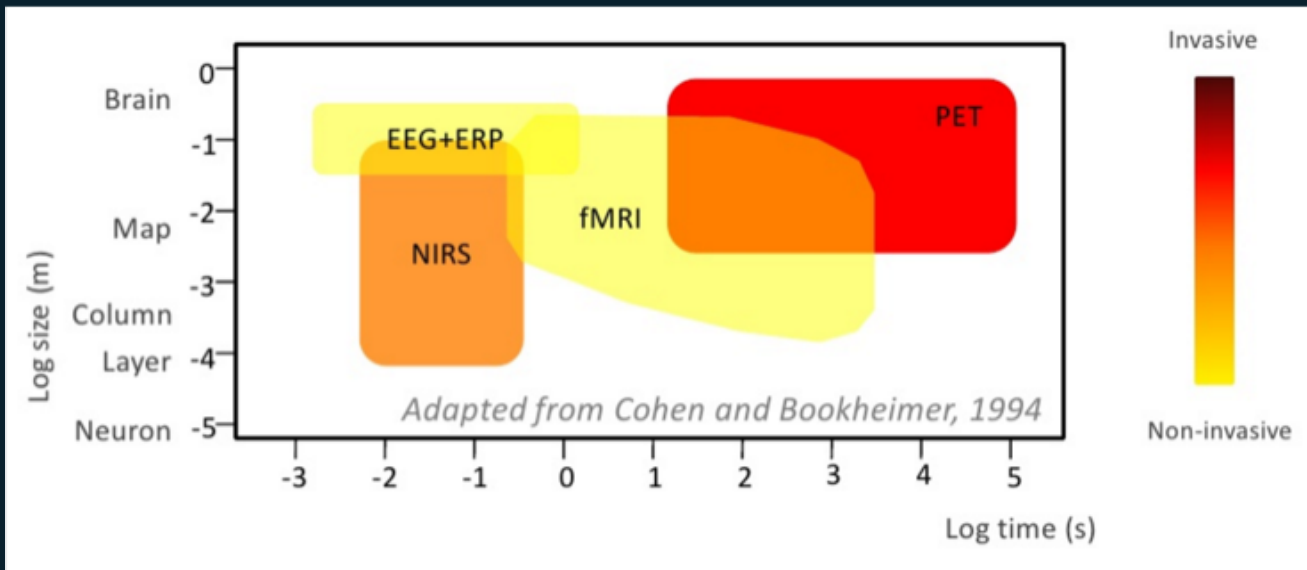


Neuroimaging Techniques



Multi-Modal Brain Imaging

- Combining multiple imaging modalities-monitor brain function at different levels
 - Direct measure of neuronal activity: ECoG, **EEG**, MEG
 - Indirect measure of neuronal activity: PET, fMRI, **fNIRS**
- Advantage:
 - enhance temporal/spatial resolutions
 - Investigate brain function from different perspectives

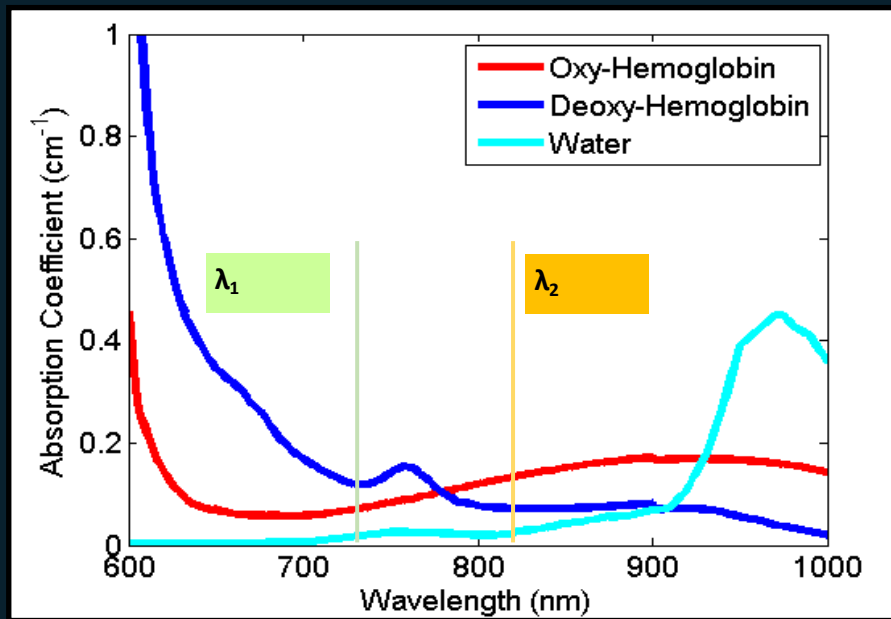
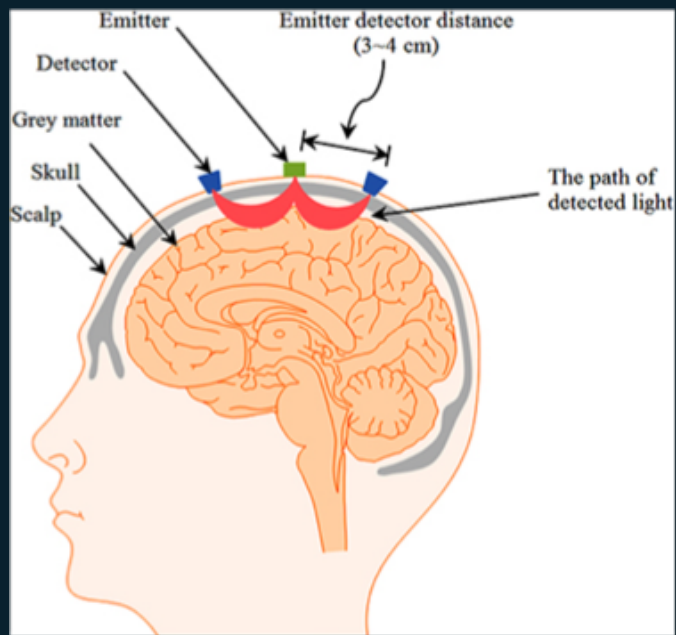


Neuroimaging Techniques



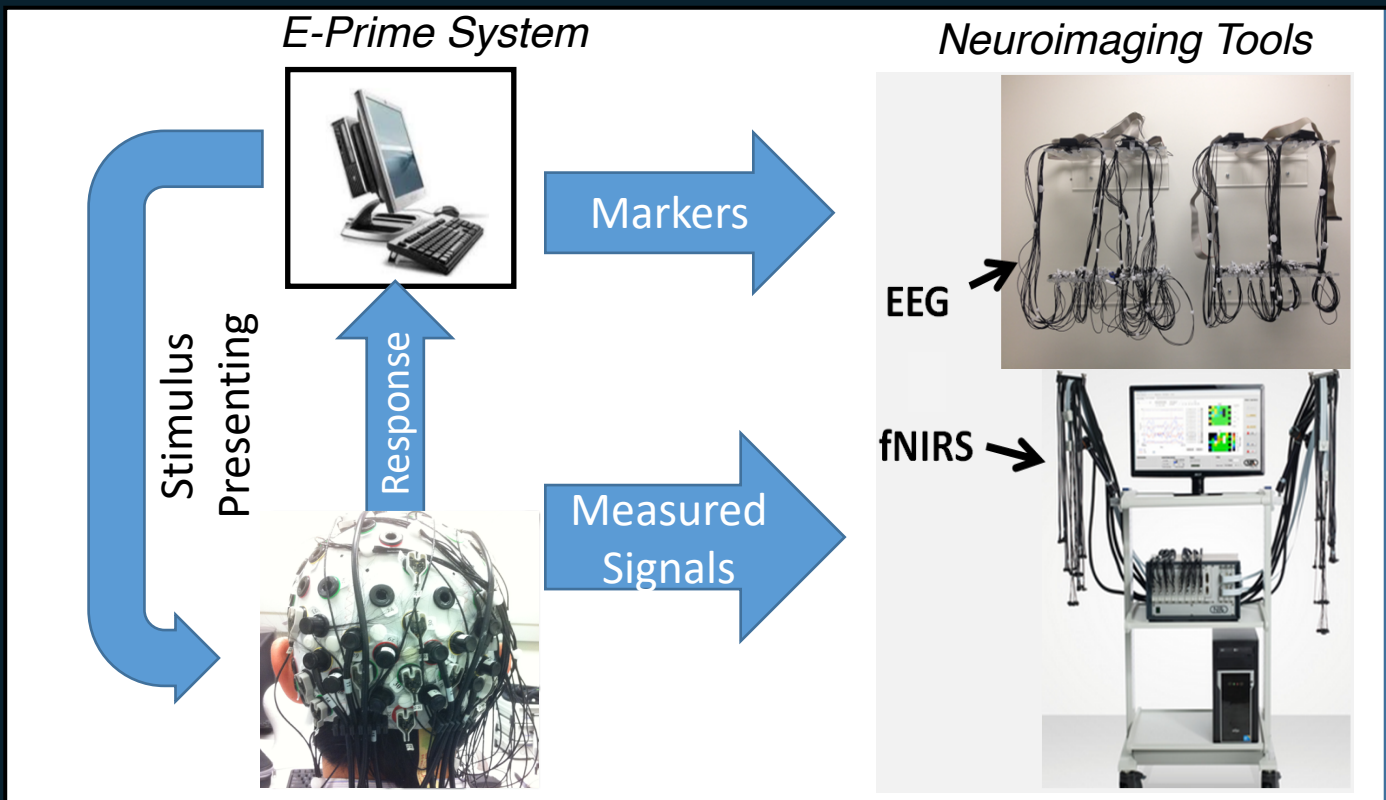
Functional Near-Infrared Spectroscopy (fNIRS)

- Diffused photons travel between source and detector
- Depth depends on the distance between source and detector



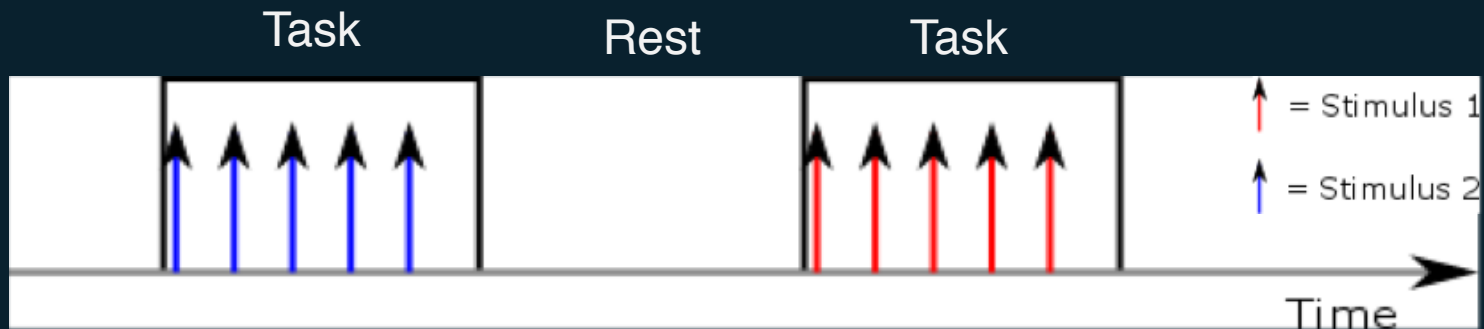
Neuroimaging Techniques

Experimental Design

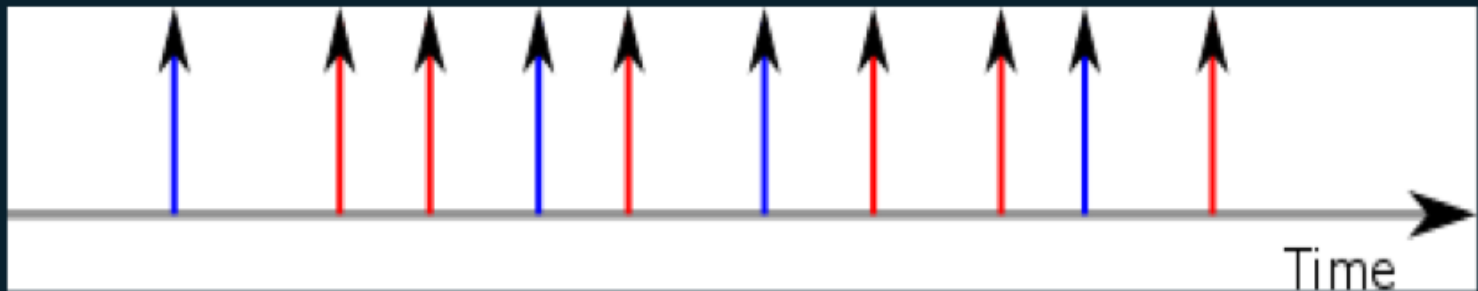


Neuroimaging Techniques

Block Design



Event-Related Design



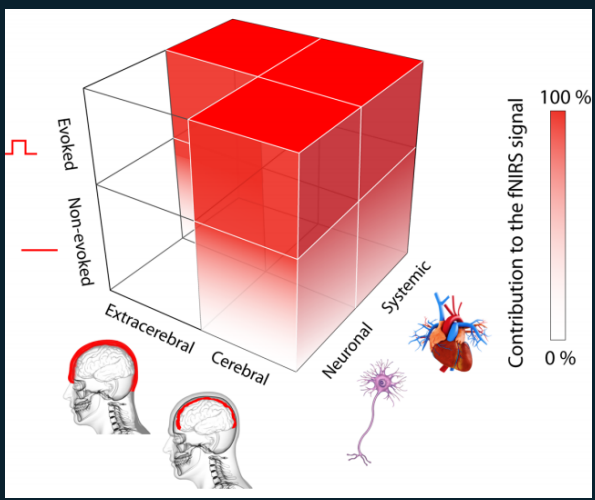


Outline

- Introduction
- Problem Statement
- Averaging Strategies - Prior Work
- Framework for DTW-based Averaging
- Experiments and Results
- Conclusion

Problem Statement

- fNIRS signal is contaminated by the physiological and measurement noise
 - Heart rate (~1 Hz)
 - Respiration (~0.3 Hz)
 - Mayer waves (~0.1 Hz)
 - Very low frequency oscillation (<0.1 Hz)
- The frequency bands of some interference components coincide with the task-evoked components, where filtering cannot be performed
- Conventional-based averaging is a routing operation for preprocessing to increase signal-to-noise-ratio





Problem Statement

Conventional-based Averaging

- Denote $\mathbf{b}_k = [b_k(1), \dots, b_k(N)]$ as the k^{th} hemodynamic signal of a group of K signals that occurs in response to a certain external stimulus
- \mathbf{b}_k can be decomposed as a summation of two components

$$b_k(n) = h(n) + e_k(n), \quad n = 1, 2, \dots, N.$$

where $h(n)$: the task-evoked hemodynamic response.

$e_k(n)$: noise

- Conventional-based averaging is performed by

$$c(n) = \frac{\sum_{k=1}^K b_k(n)}{K}$$

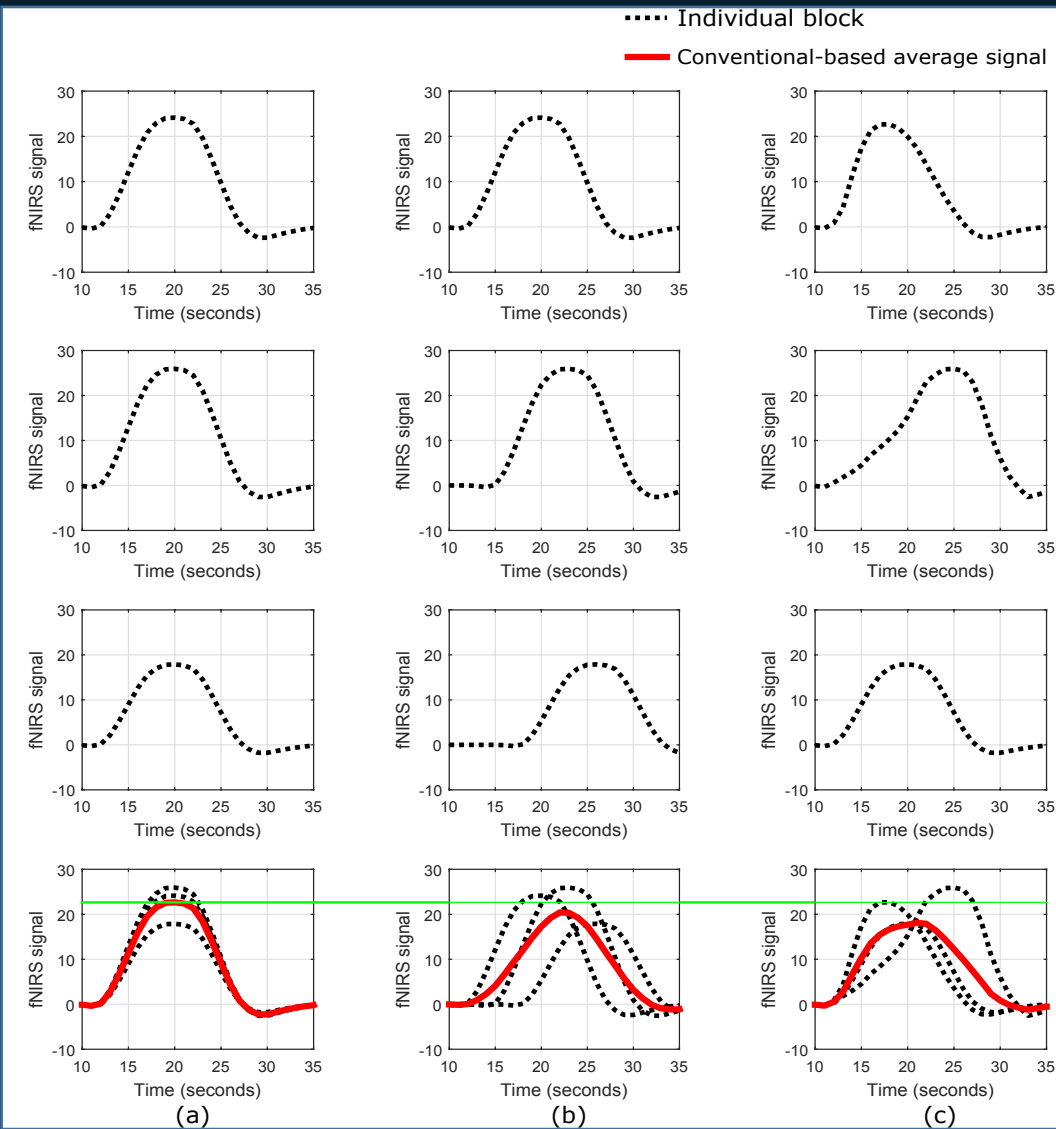


Problem Statement

Problems with Conventional-based Averaging

- The invariant assumption on $h(n)$ in the brain responses does not always hold
- Trial-to-trial variability of the brain response is observed in EEG measurements
- Hemodynamic signals are indirect measure of the neural activities, via neurovascular coupling. Therefore, it is expected that they also experience trial-to-trial variable latency
- Performing conventional-based averaging might lead to a blurring (or loss) of peaks and valleys in the averaged signal

Problem Statement





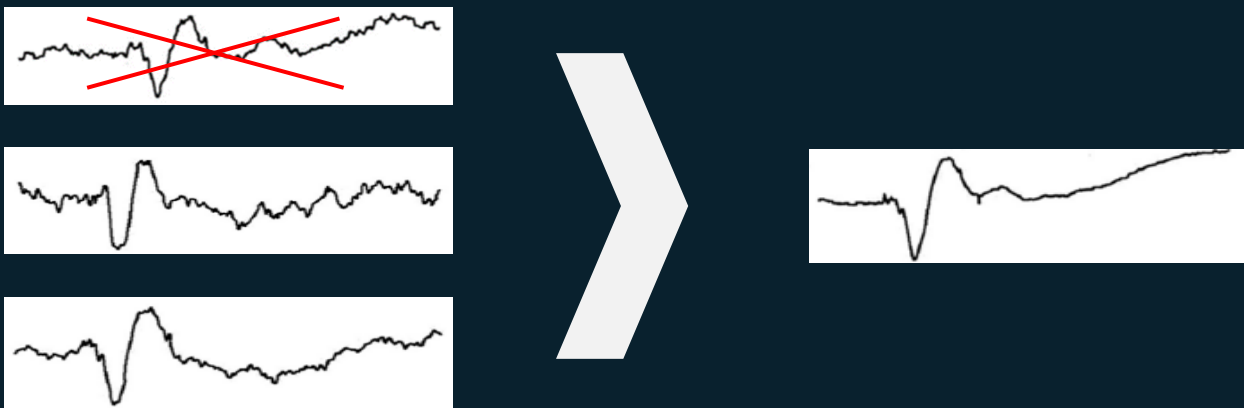
Outline

- Introduction
- Problem Statement
- Averaging Strategies - Prior Work
 - Conventional-based Averaging
 - Selective Averaging
 - Linear Alignment Averaging
 - Non-linear Alignment Averaging
- Framework for DTW-based Averaging
- Experiments and Results
- Conclusion

Literature Review

Selective Averaging

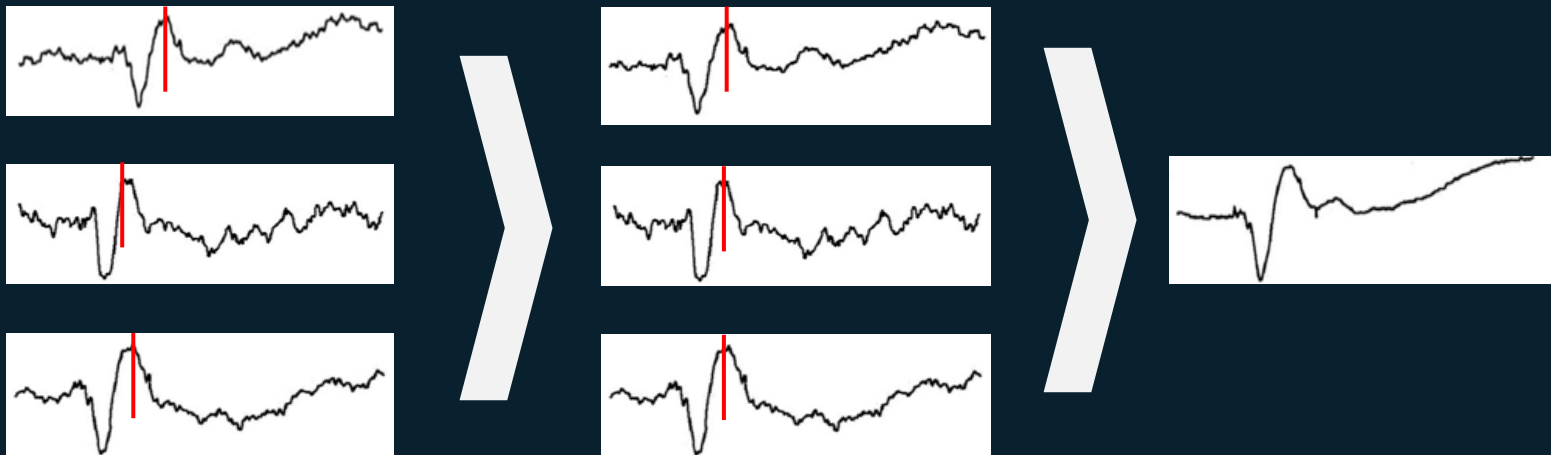
- Goal: task-related signals in some individual blocks/trials may not be obtained, and should be excluded from the averaging process
- Visually inspection



Literature Review

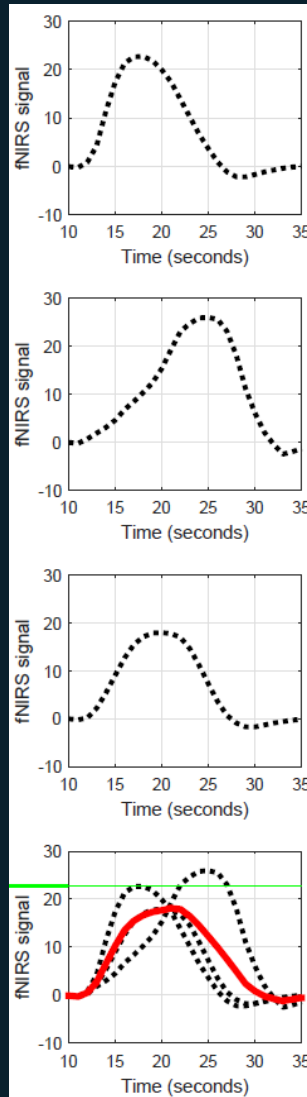
Linear Alignment Averaging

- Alternative model for measured signals
$$\mathbf{b}_k(n) = h(n + \Delta\tau_k) + e_k(n), \quad n = 1, 2, \dots, N$$
- Methods for estimating the latency exists
 - Cross-correlation



Literature Review

How about scenarios where individual blocks/trials experience *non-linear* distortion?

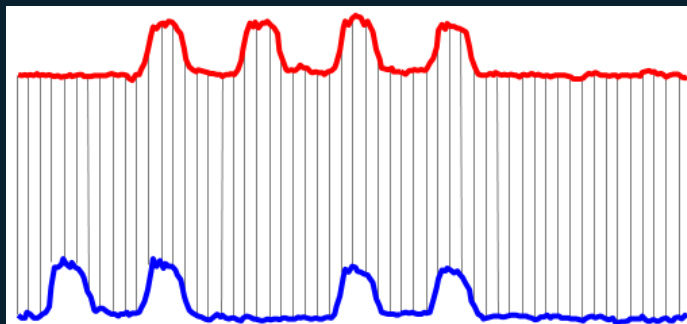


Literature Review

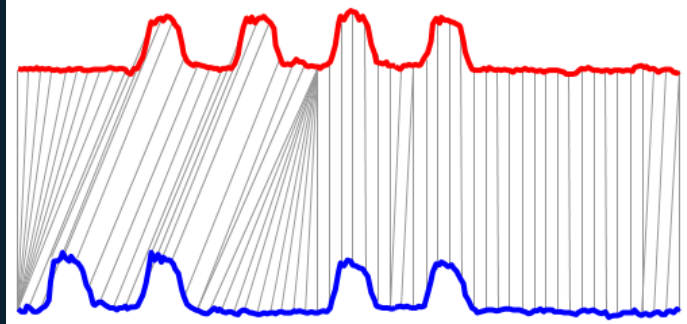
Non-linear Alignment Averaging

- Aligning using dynamic time warping
- Application: speech processing or pattern recognition

Aligning point-to-point



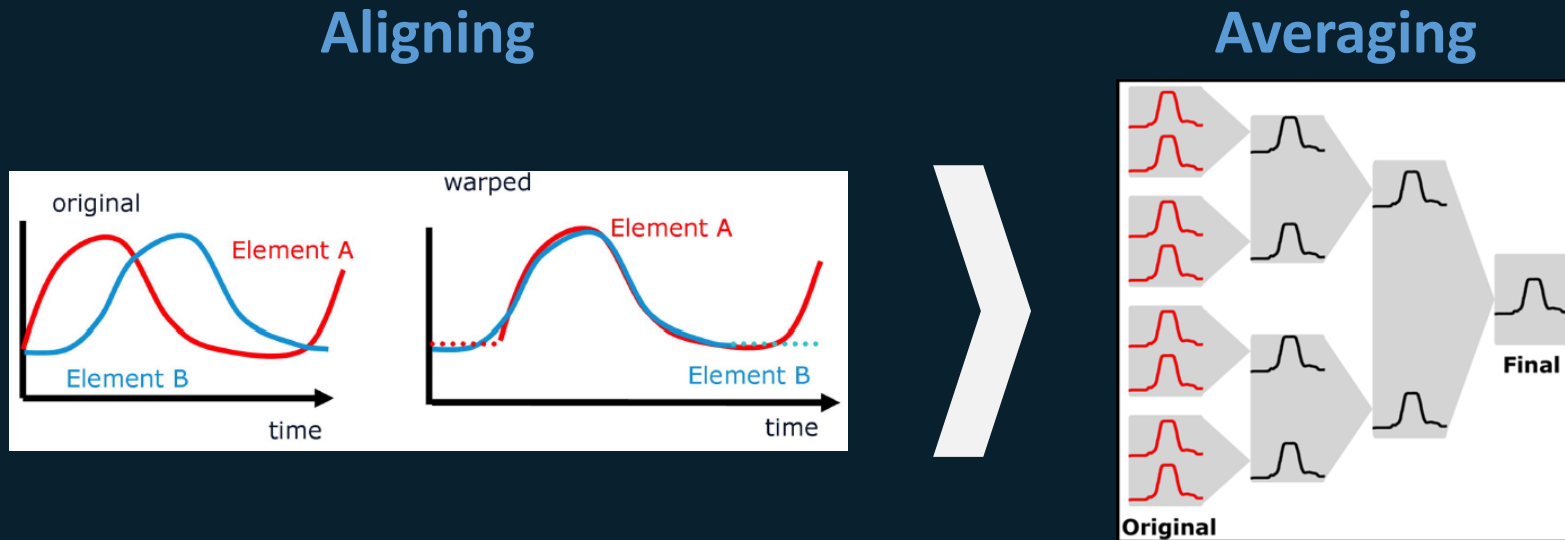
Non-linear alignment



Literature Review

Non-linear Alignment Averaging

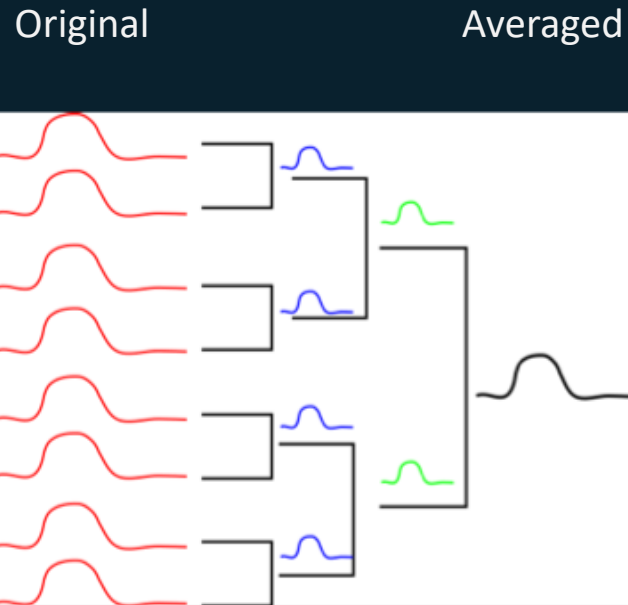
- Aligning using dynamic time warping
- Application: ERP, speech processing or pattern recognition



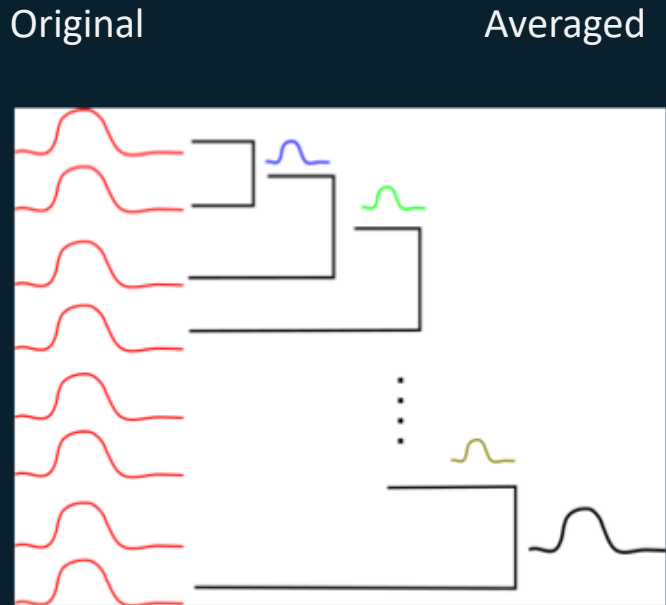
DTW-based Averaging

Strategies Used

Pair-wise Alignment Averaging



Sequential Alignment Averaging

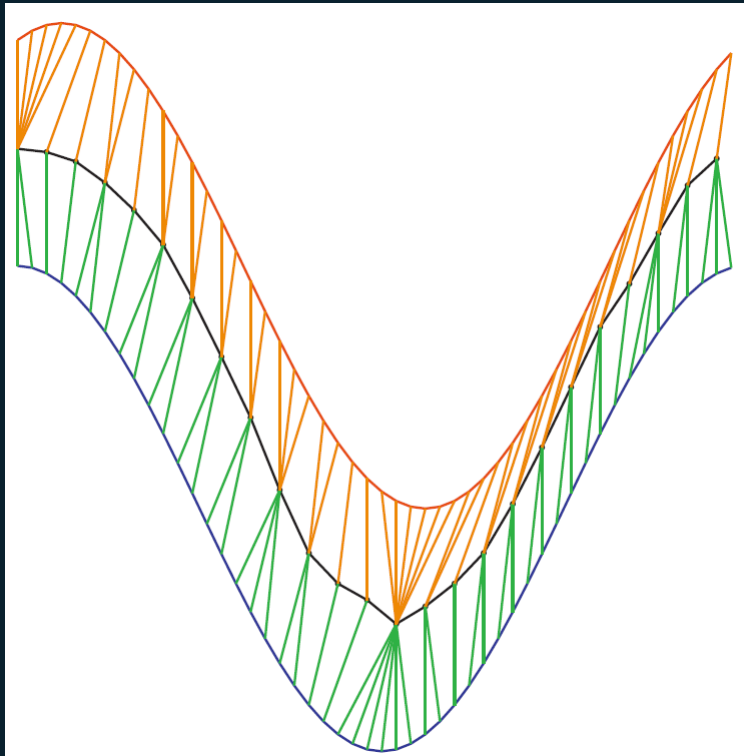


DTW-based Averaging



Strategy Used in This Study

Simultaneous Alignment Averaging





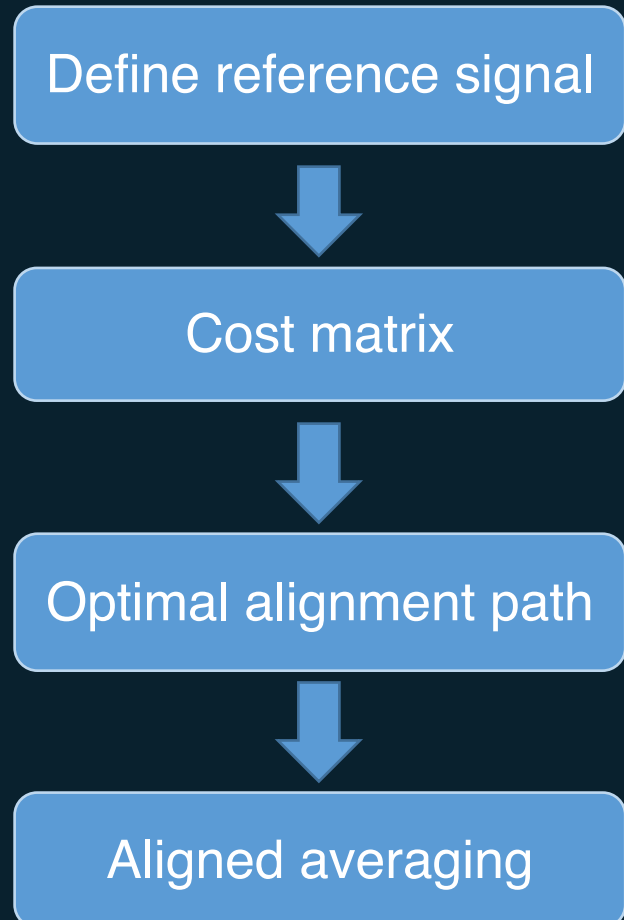
Outline

- Introduction
- Problem Statement
- Averaging Strategies - Prior Work
- Framework for DTW-based Averaging
- Experiments and Results
- Conclusion



DTW-based Averaging

Overview



Define a reference signal c

Between individual signal b_k and c

For b_k , find optimal alignment path to c

Find the output signal based on the optimal alignment paths



DTW-based Averaging

Procedure



- Denote $b_k = [b_k(1), \dots, b_k(N)]$ as the k^{th} hemodynamic signal of a group of K signals that occurs in response to a certain external stimulus.
- In this study, we consider the “*reference*” signal to be the point-by-point arithmetic average of all K signals denoted as $c = [c(1), c(2), \dots, c(N)]$,

$$\text{where } c(n) = \frac{\sum_{k=1}^K b_k(n)}{K}, \quad n = 1, 2, \dots, N.$$

DTW-based Averaging

Procedure

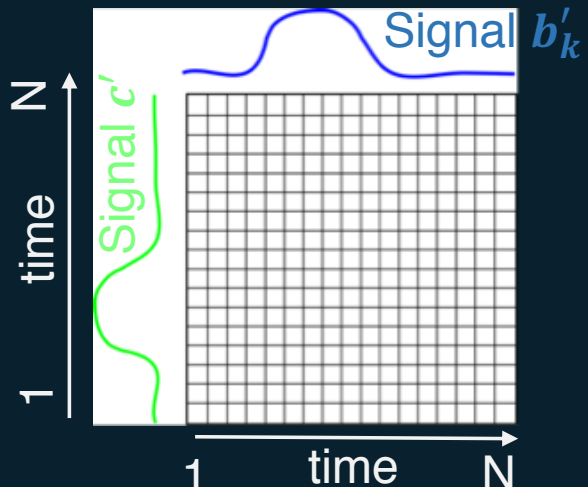


- Normalize c and b_k for each $k = 1, 2, \dots, K$

$$b'_k = \frac{b_k - \mathbb{E}(b_k)}{\sigma_{b_k}}, \quad c' = \frac{c - \mathbb{E}(c)}{\sigma_c}.$$

- For each b'_k , establish the Cost Matrix D_k

$$D_k(i, j) = (c'(i) - b'_k(j))^2$$



DTW-based Averaging

Procedure

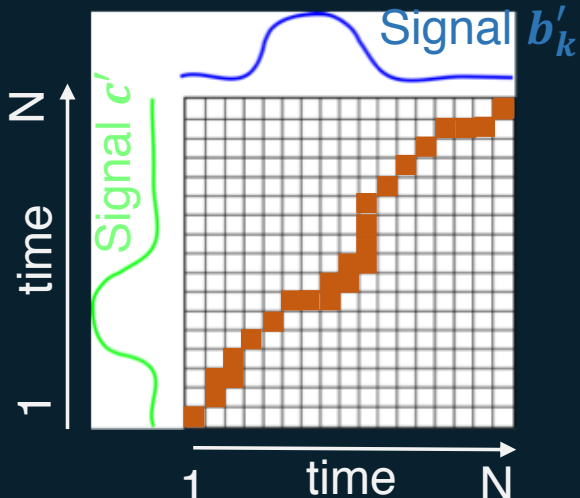


- To find $\mathbf{W}_k^{opt} = [w_1, \dots, w_l, \dots, w_L]^T$, $N \leq L \leq 2N - 1$, where $w_l = (i_l, j_l)$, $1 \leq i_l, j_l \leq N$, i_l and j_l are the indices on the signals c' and b'_k associated to the l^{th} path step, respectively
- We seek the solution for the following problem

$$\underset{\mathbf{W}_k}{\text{minimize}} \sum_{l=1}^L D_k(i(l), j(l)),$$

Subject to the following constraints:

- Monotonicity alignment*
- Continuity*
- End-point alignment*



DTW-based Averaging

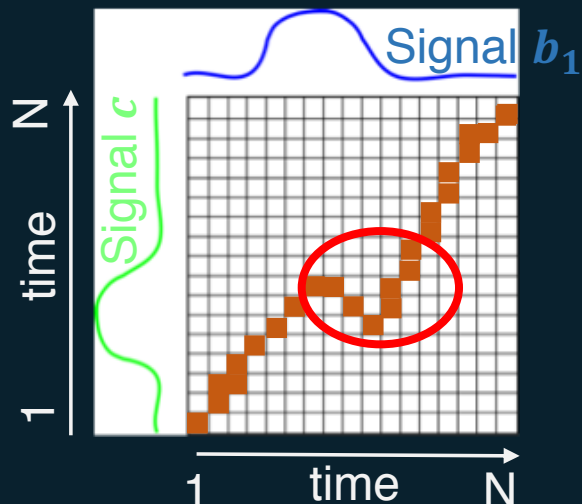
Procedure



Constraints:

- Monotonicity alignment: regularizes the alignment path does not go back in time index

$$i(l) \geq i(l - 1), \text{ and } j(l) \geq j(l - 1)$$



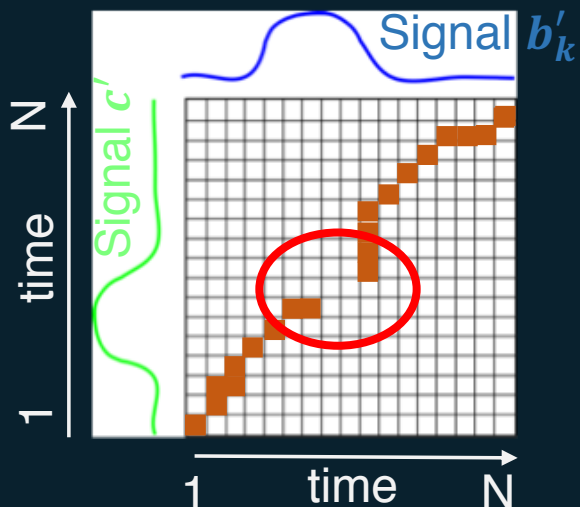
DTW-based Averaging

Procedure



Constraints

- Continuity: regularizes the alignment path does not jump in time index
 $i(l) - i(l - 1) \leq 1$, and $j(l) - j(l - 1) \leq 1$



DTW-based Averaging

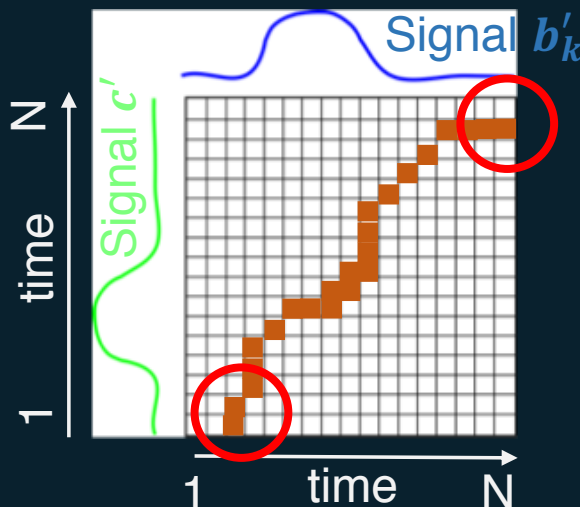
Procedure



Constraints

- End-point alignment: requires the alignment path to start at the bottom left and ends at the top right

$$i(1) = j(1) = 1, \text{ and } i(L) = j(L) = N$$



DTW-based Averaging Procedure



Update b_k according to W_k^{opt}

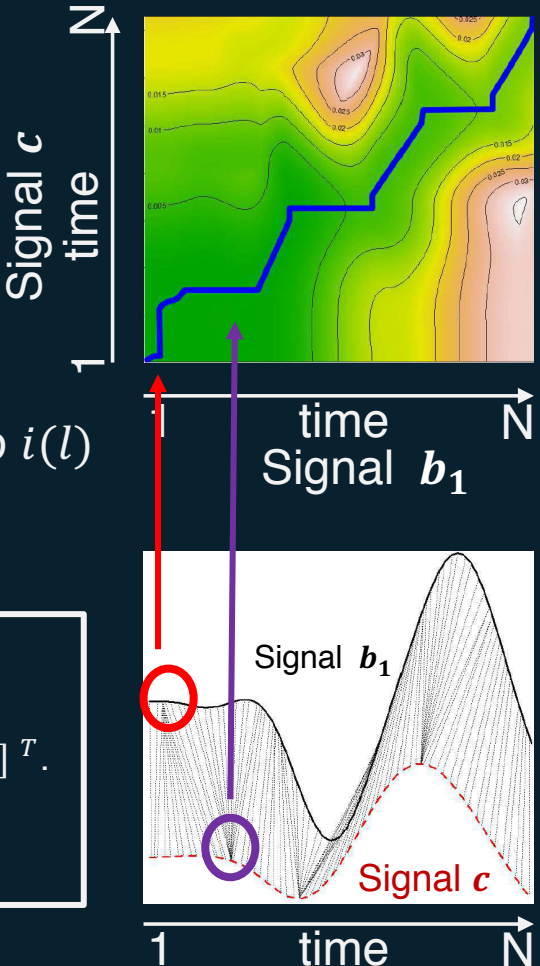
- If the index represented by $i(l)$ is unique in W_k^{opt} ,
 $b_{k(aligned)}(m) = b_k(j(l))$
- If the index represented by i_l is not unique in W_k^{opt} ,
 $b_{k(aligned)}(m) = \text{average of all } b_k(j(l))\text{'s corresponding to } i_l$

Example

Index on c Index on b

Assume that $W_k^{opt} = [(1,1), (2,2), (2,3), (2,4), (3,5), \dots, (N-1, N-1), (N, N)]^T$.

Then $b_{k(aligned)} = [b_k(1), \frac{b_k(2)+b_k(3)+b_k(4)}{3}, \dots, b_k(N)]$.





DTW-based Averaging

Procedure



- After determining $\mathbf{b}_{k(aligned)}$ for all $k = 1, 2, \dots, K$, the DTW-based average is obtained as

$$\mathbf{b}_{\text{DTWaveraged}} = \frac{\sum_{k=1}^K \mathbf{b}_{k(aligned)}}{K}$$



Outline

- Introduction
- Problem Statement
- Averaging Strategies - Prior Work
- Framework for DTW-based Averaging
- Experiments and Results
 - Experiment I
 - Experiment II
 - Simulation Study
- Conclusion



Experimental Studies

- **Experiment I**

- Block-design experiment - *N-back tasks*
- Investigate detection power in identifying active regions

- **Experiment II**

- Event-related design experiment - *modified visual odd-ball task*
- Identify brain regions sensitive to the contrast effect

- **Simulation Study**

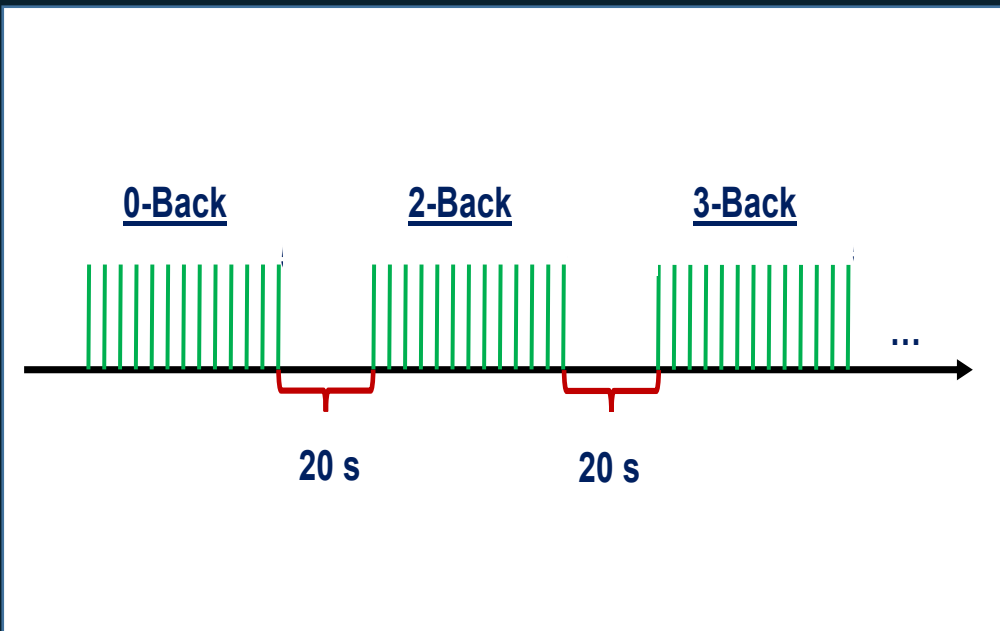
- Data sets simulated based on the same task as Experiment II
- Ground truth is known
- Investigate false positive rate in identifying brain regions sensitive to the contrast effect

Experiment I

Task Paradigm: Block Design

N-Back (N=0, 2, 3)-Working Memory

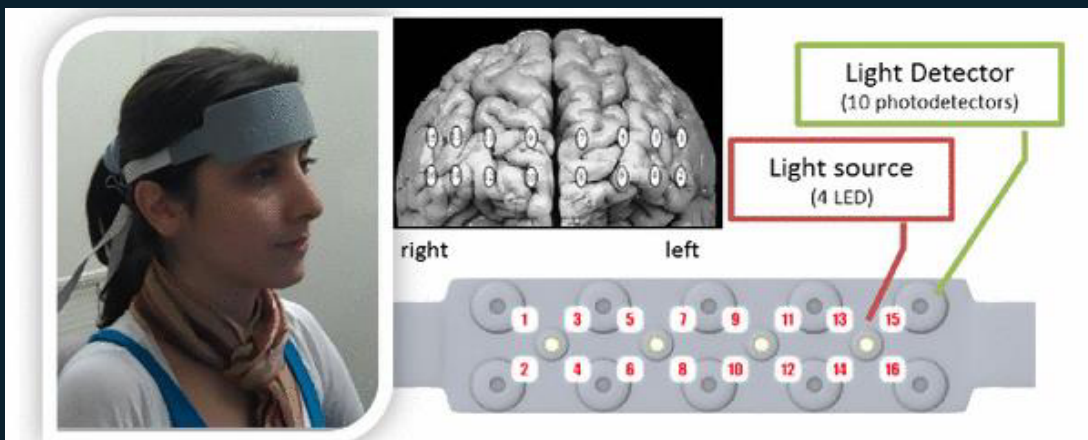
- 4 blocks for each N-Back
- 15-stimuli in each block
- ITI=2 s
- Left click if see target



Experiment I

Data Acquisition

- 10 healthy volunteers
- BIOPAC fNIR system
- 4 sources, 16 detectors
- 16 channels
- Cover prefrontal cortex
- 730 nm and 850 nm
- Sampling rate: 2 Hz
- Spatial Resolution: 2.5 cm



Experiment I

- Extracting Brain Activities

- both ΔHbO_2 and ΔHbR were extracted using Modified Beer Lambert Law:

Wavelength 1 (760 nm): $\ln\left(\frac{I_{\text{task},\lambda_1}}{I_{\text{baseline},\lambda_1}}\right) = -(\epsilon_{HbO_2,\lambda_1} \Delta C_{HbO_2} + \epsilon_{HbR,\lambda_1} \Delta C_{HbR}) \cdot L_{\lambda_1}$

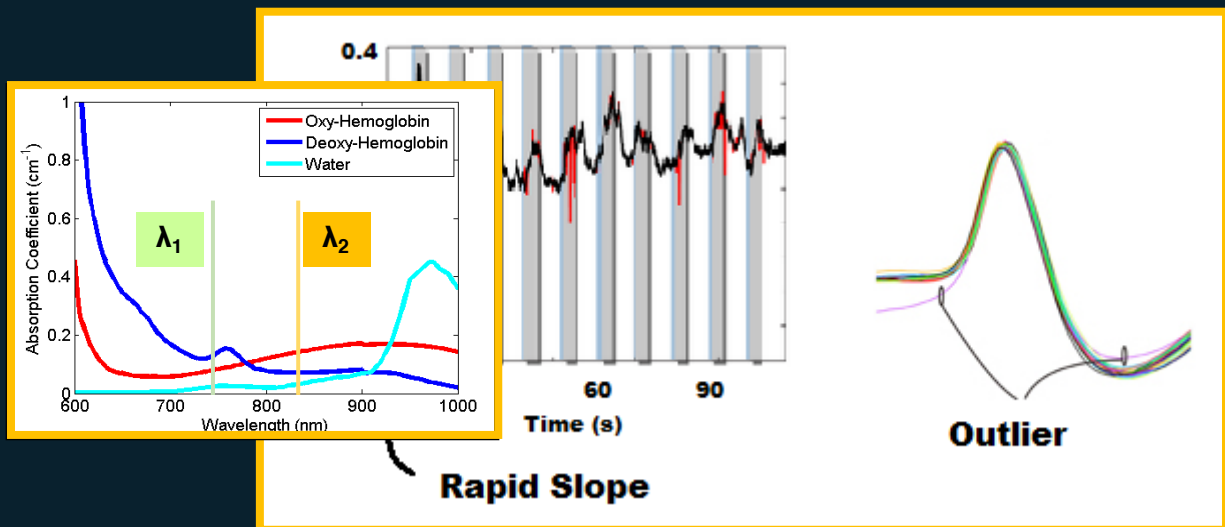
Wavelength 2 (830 nm): $\ln\left(\frac{I_{\text{task},\lambda_2}}{I_{\text{baseline},\lambda_2}}\right) = -(\epsilon_{HbO_2,\lambda_2} \Delta C_{HbO_2} + \epsilon_{HbR,\lambda_2} \Delta C_{HbR}) \cdot L_{\lambda_2}$

- Band-pass filtering

- Artifacts rejection

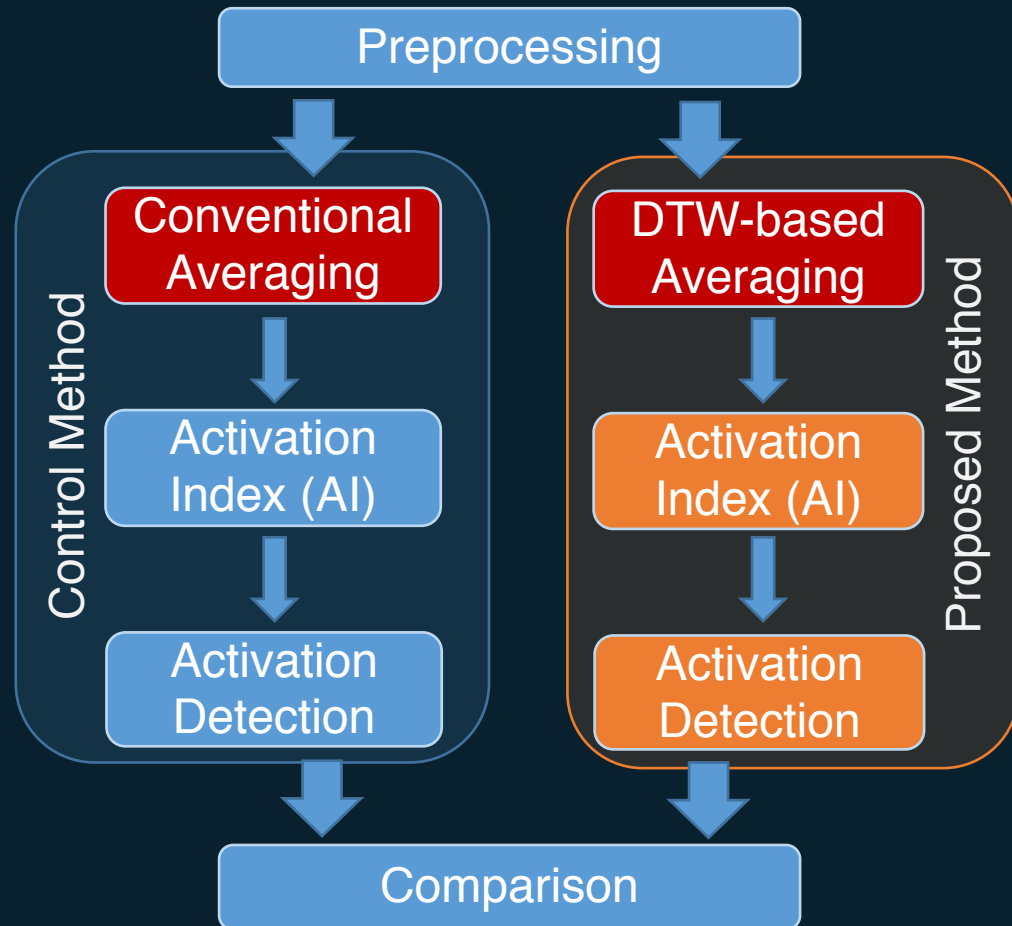
- Rapid slope

- Outlier



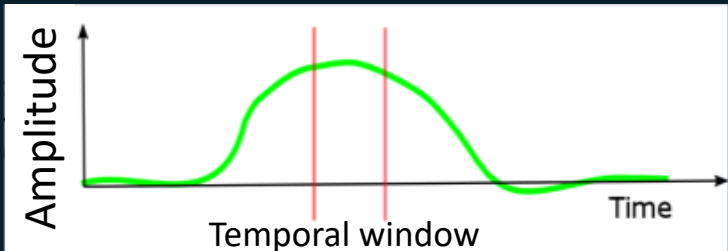
Experiment I

Analysis Procedure



- Extraction of HbO_2
- Filtering
- Baseline correction
- Segmentation

Conventional- and DTW-based averaging techniques were conducted on ΔHbO_2 signals across blocks separately.

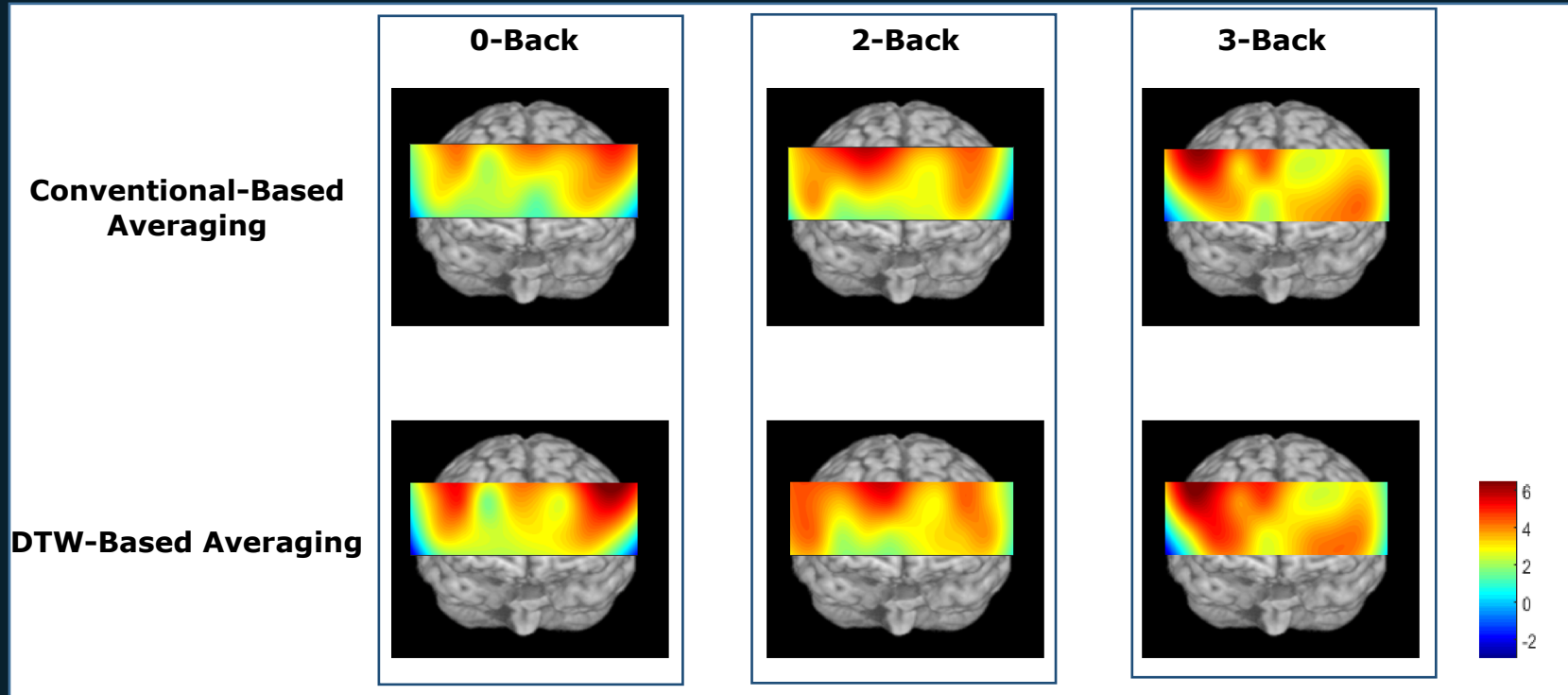


Channel-wise one sample t-tests were performed on AI with null hypothesis being the region is not active.

Experiment I

Detection Power

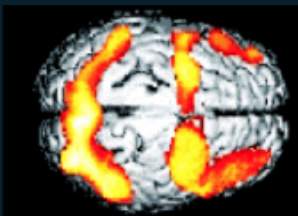
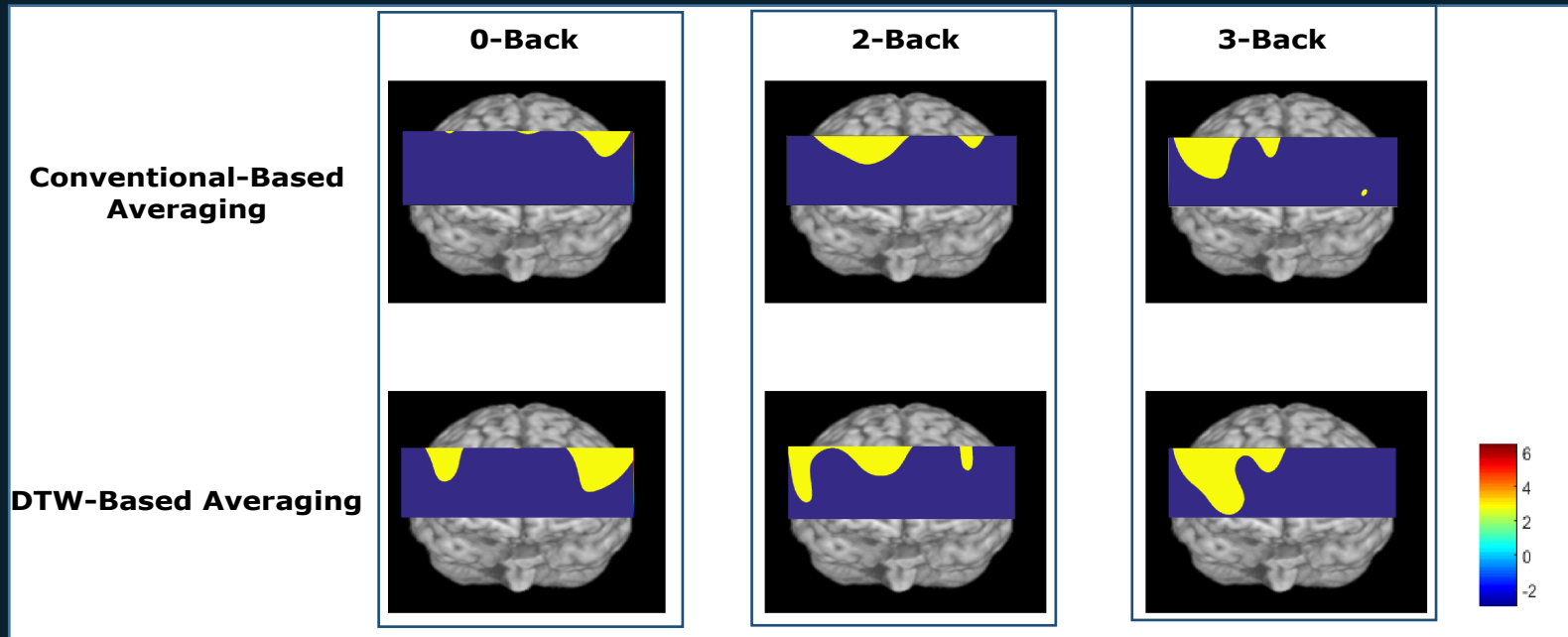
- Statistical activation map for N-back tasks.



Experiment I

Detection Power

- Statistical activation map thresholded by the significant level of $p < 0.001$.



M. Glabus et al., 2003



Experiment I

CNR

- Contrast-to-noise-ratio (CNR): a metric used for quantifying the signal-to-noise-ratio.
- $CNR = \frac{|mean(dur) - mean(ITI)|}{\sqrt{var(dur) + var(ITI)}}.$

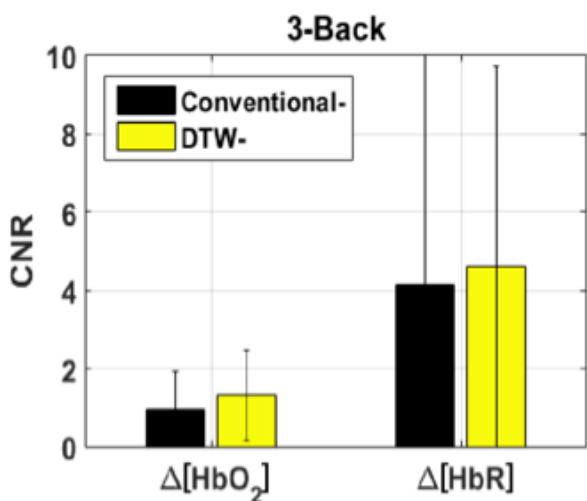
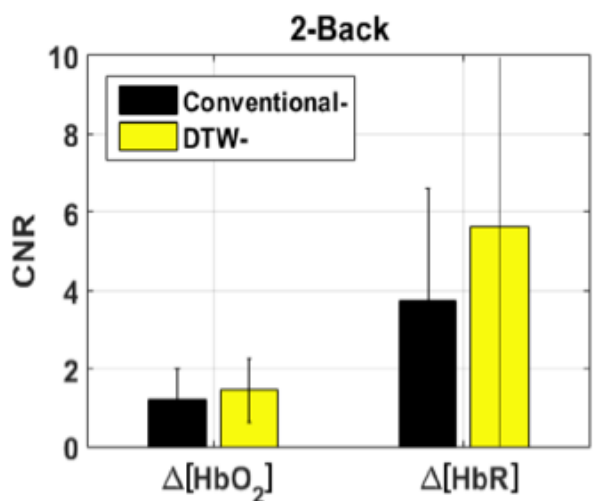
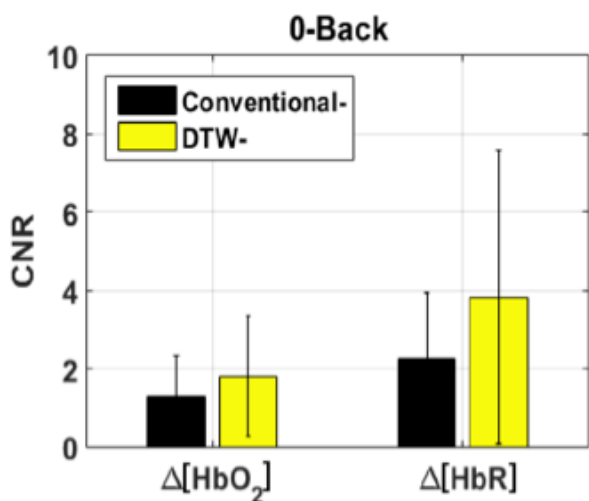
Dur: the signal corresponding to 5-20 s after the presentation of the first stimulus of a block.

ITI: the signal corresponding to 10-15 s after the presentation of the last stimulus of a block.

Experiment I

CNR

Mean CNR computed from DTW-based averaging is significantly higher for all conditions.





Experimental Studies

- **Experiment I**

- Block-design experiment - *N-back tasks*
- Investigate detection power in identifying active regions

- **Experiment II**

- Event-related design experiment - *modified visual odd-ball task*
- Identify brain regions sensitive to the contrast effect

- **Simulation Study**

- Data sets simulated based on the same task as Experiment II
- Ground truth is known
- Investigate false positive rate in identifying brain regions sensitive to the contrast effect

Experiment II

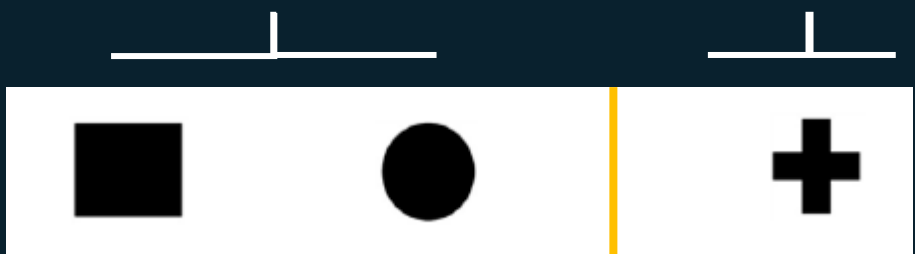
Task Paradigm: Event–Related Design

Modified Visual Odd Ball Task: Attention, Surprise Effect

- 30 target trials
- 190 frequent stimuli trials
- Presentation time = 50 ms
- ITI = 10 – 12 s
- Left click if see target
- 5 healthy participants

Target
Odd-ball stimuli

Frequent stimuli



Frequent
stimuli

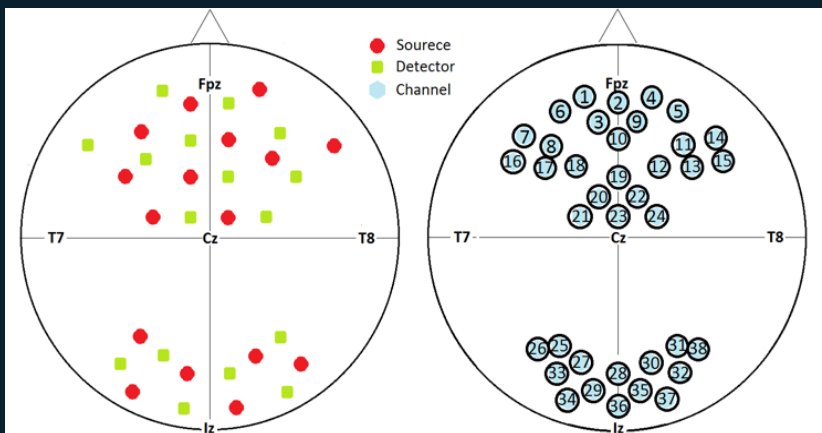
Surprise
stimuli



Experiment II

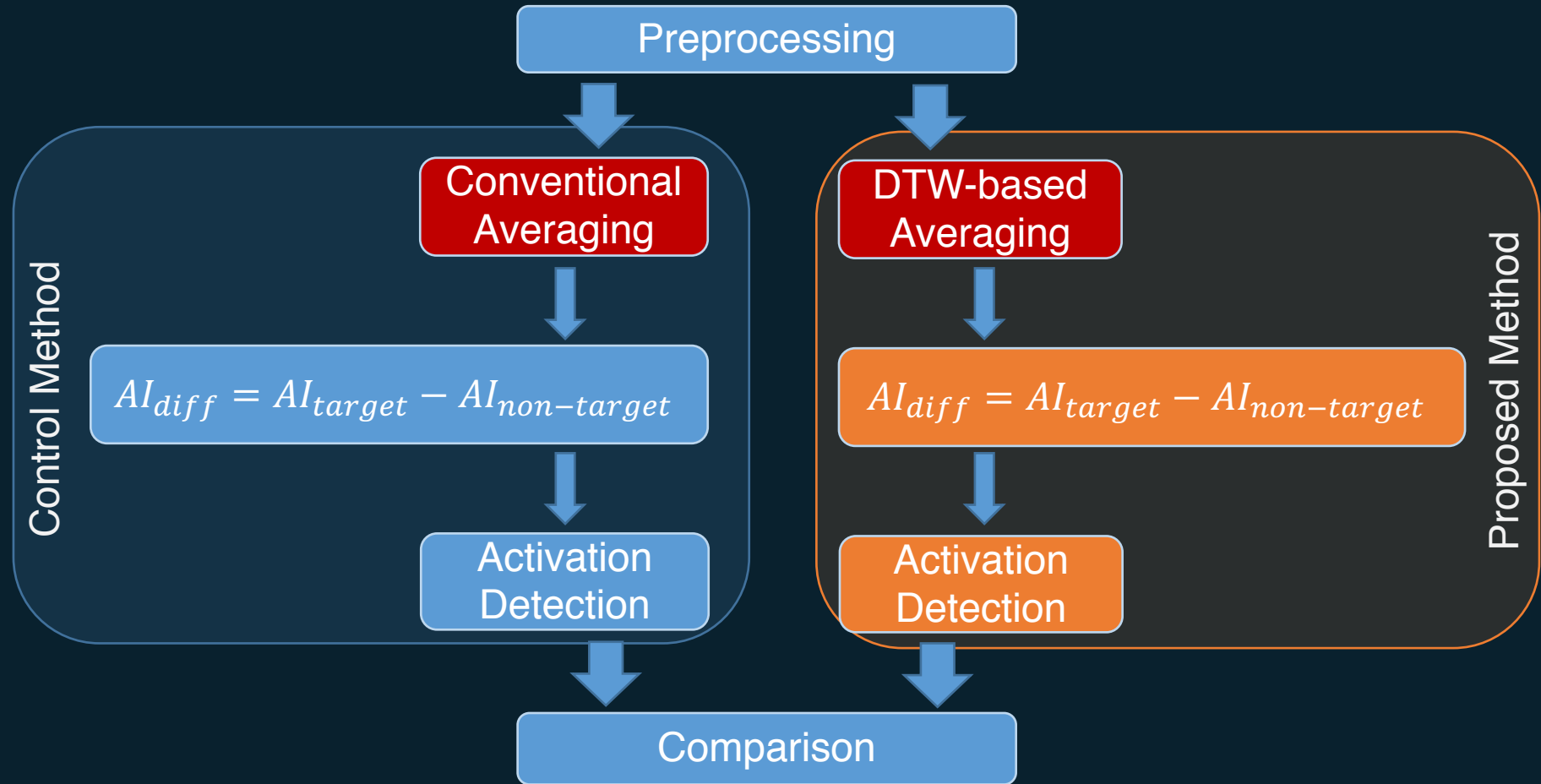
Data Acquisition

- 6 healthy volunteers
- NIRx NIRScout system
- 16 sources, 16 detectors
- 38 channels
- cover prefrontal/visual cortices
- 760 and 830 nm
- Sampling rate: 10.42 Hz
- Spatial Resolution: 3 cm
- Stimuli Sent by E-prime



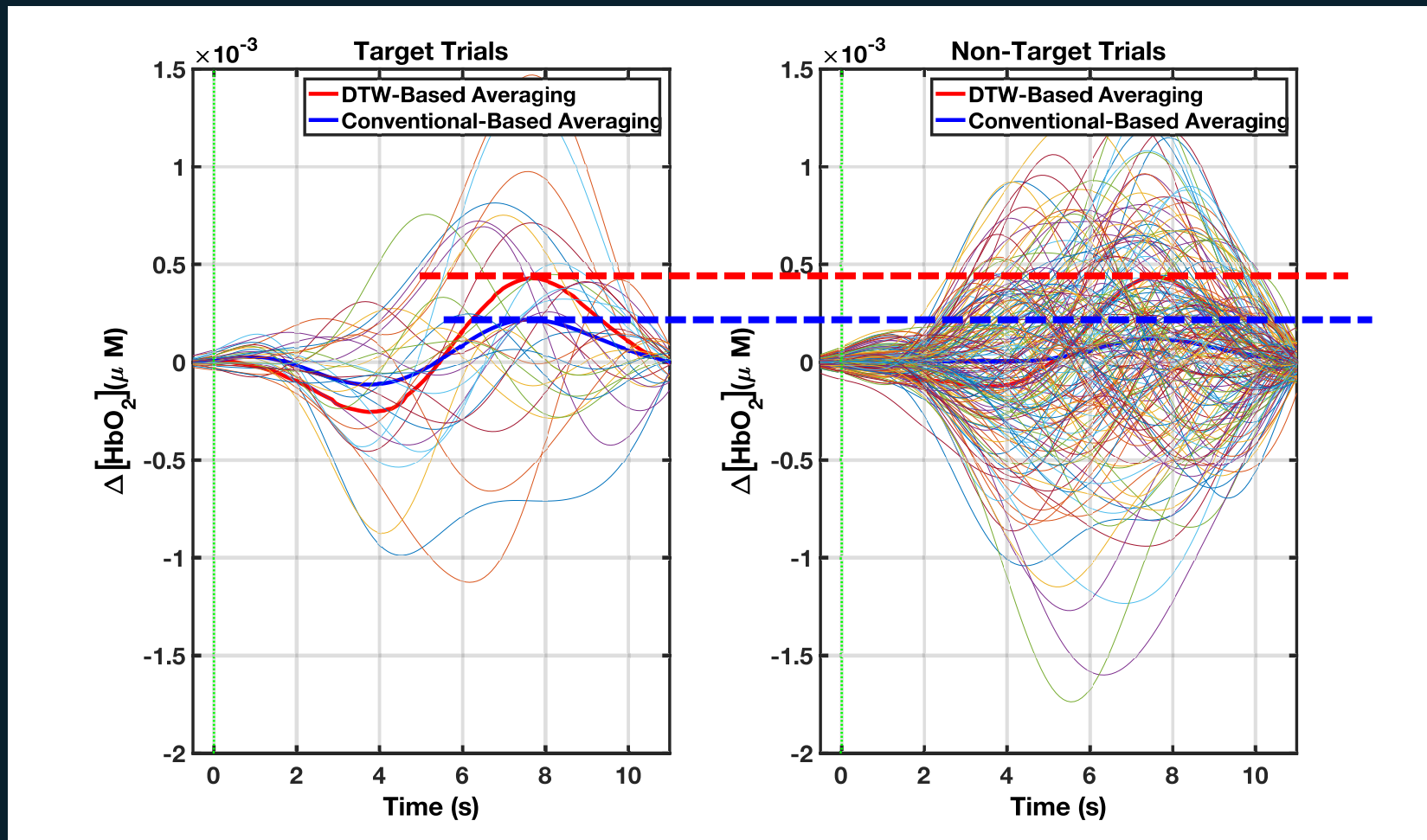
Experiment II

Analysis Procedure



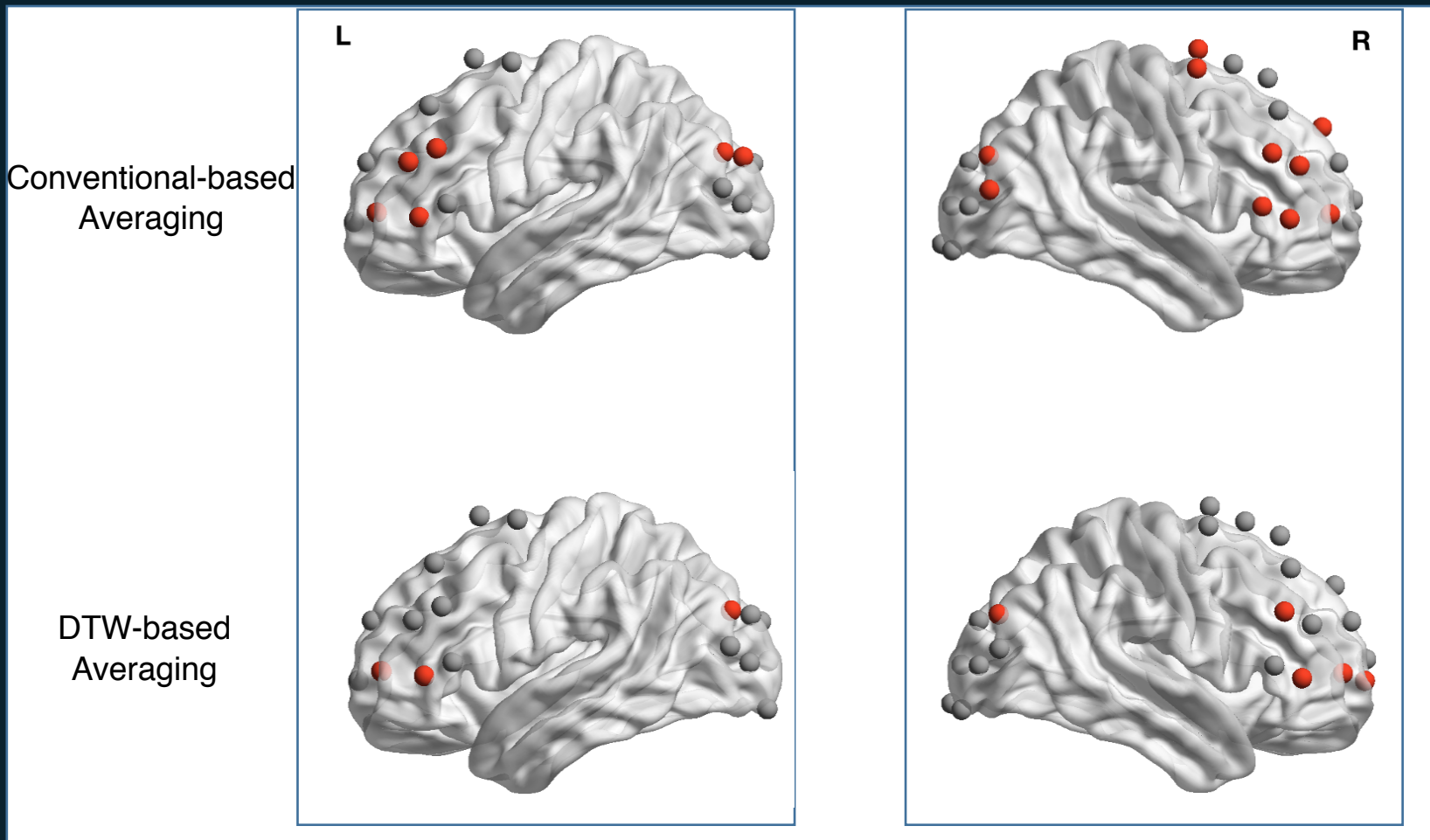
Experiment II

Exemplary recorded signals from a given channel for two conditions



Experiment II

Red channels are specifically sensitive to rare interruption ($p < 0.05$)





Experimental Studies

- **Experiment I**

- Block-design experiment - *N-back tasks*
- Investigate detection power in identifying active regions

- **Experiment II**

- Event-related design experiment - *modified visual odd-ball task*
- Identify brain regions sensitive to the contrast effect

- **Simulation Study**

- Data sets simulated based on the same task as Experiment II
- Ground truth is known
- Investigate false positive rate in identifying brain regions sensitive to the contrast effect



Simulation Study

Simulation Platform

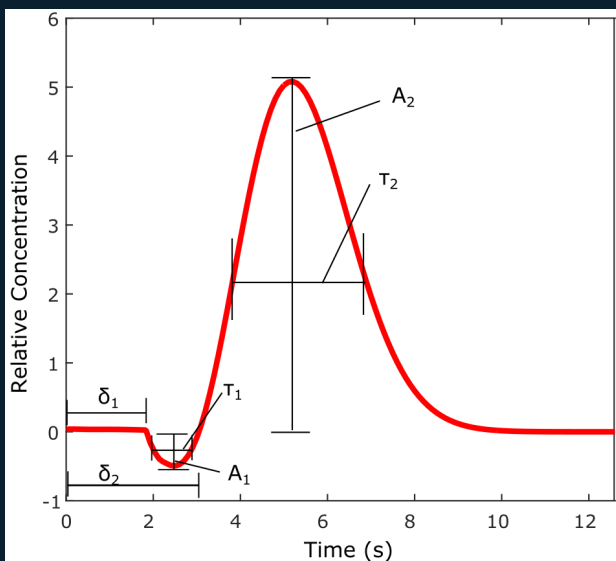
- Datasets are simulated under the framework of visual odd ball task
 - 50-channel fNIRS recordings
 - 10 channels are sensitive to the contrast (target > non-target) effect
 - 40 channels are sensitive to both conditions, but are not sensitive to the contrast effect
 - 20 target trials
 - 150 non-target trials
 - 40 subjects
- Objective: identify the 10 channels sensitive to the contrast effect

Simulation Study

- The hemodynamic response is simulated based on the widely used double gamma function [61]

$$HRF(t, \tau_1, \tau_2, \delta_1, \delta_2, c_1, c_2) = c_1 \left(\frac{t-d}{\tau_1}\right)^{\delta_1} \exp^{-(\delta_1/\tau_1)(t-\tau_1)} - c_2 \left(\frac{t-d}{\tau_2}\right)^{\delta_2} \exp^{-(\delta_2/\tau_2)(t-\tau_2)},$$

where c_1 and c_2 model the amplitude of the undershoot and the peak,
 δ_1 and δ_2 model the shape of the gamma functions,
 τ_1 and τ_2 model the width of the gamma functions





Simulation Study

- The hemodynamic response is simulated based on the widely used double gamma function [61]

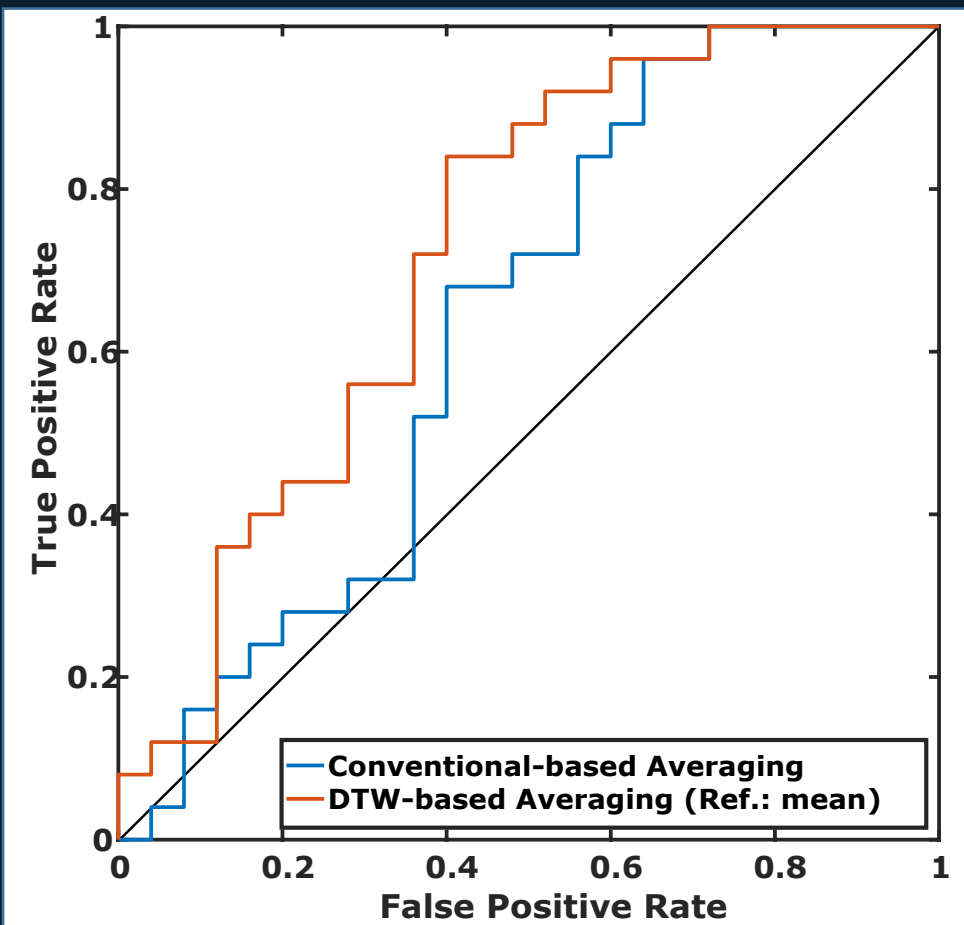
$$HRF(t, \tau_1, \tau_2, \delta_1, \delta_2, c_1, c_2) = c_1 \left(\frac{t-d}{\tau_1}\right)^{\delta_1} e^{-\delta_1/\tau_1}(t-\tau_1) - c_2 \left(\frac{t-d}{\tau_2}\right)^{\delta_2} e^{-\delta_2/\tau_2}(t-\tau_2),$$

where c_1 and c_2 model the amplitude of the undershoot and the peak,
 δ_1 and δ_2 model the shape of the gamma functions,
 τ_1 and τ_2 model the width of the gamma functions.

- τ_1 , τ_2 , and d : normally distributed random variables.
- $AMP_{TA} = 1.03 \times AMP_{NT}$.
- $SNR = 10 \text{ dB}$

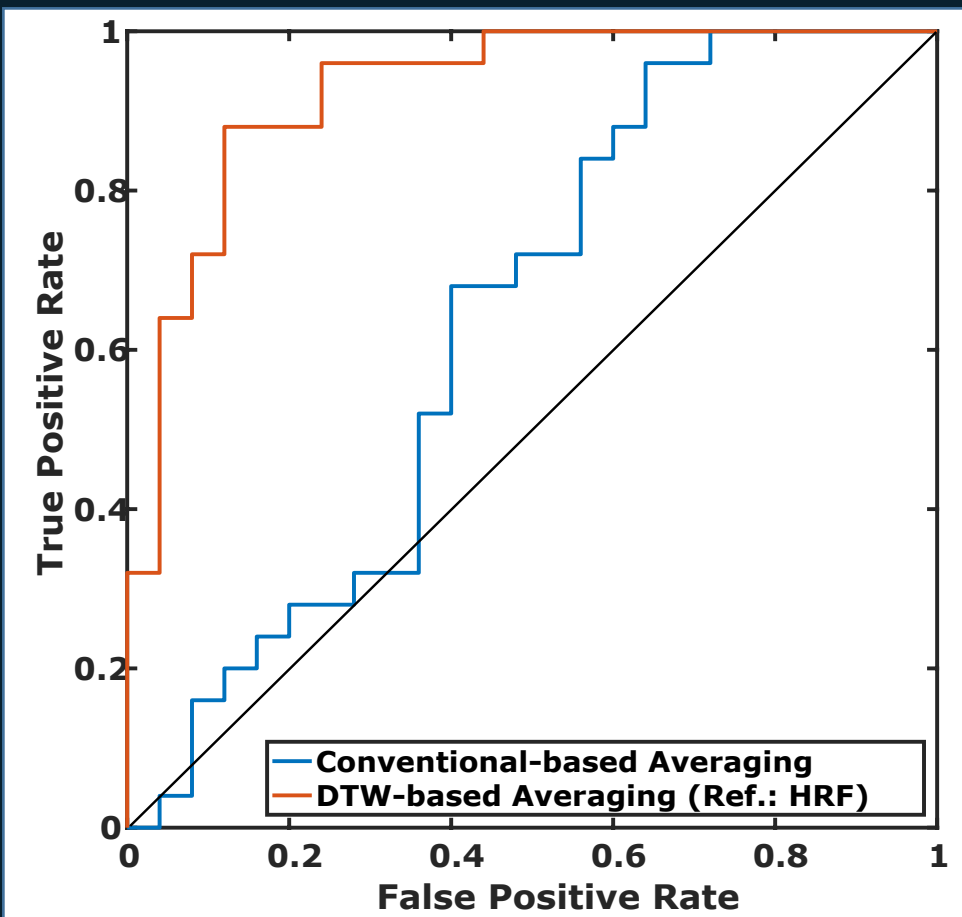
Simulation Study

- ROC curves for conventional- and DTW-based averaging
- DTW-based averaging outperforms conventional averaging



Simulation Study

- HRF was chosen as the reference signal
- DTW-based averaging outperforms conventional averaging





Conclusion

- We investigated the problem of accurately localizing active regions in the brain using fNIRS-recorded time series
- Due to the existence of trial-to-trial variability and variable latencies, the use of conventional averaging procedures may lead to loss of information in the averaged signal
- An averaging framework utilizing DTW technique is presented, aiming to improve the averaging accuracy of fNIRS signals by taking into account the nonlinearities in the alignment of signals to be averaged
- The averaging framework is extensively tested on real data, from block design and event-related design experiments, as well as on simulated data. It is shown that DTW-based averaging technique significantly outperforms the conventional-based averaging



Publication

- L. Zhu**, A. Haddad, T. Zeng, Y. Wang and L. Najafizadeh, "Assessing Optimal Electrode/Optode Arrangement in EEG-fNIRS Multi-Modal Imaging," OSA Technical Digest, Fort Lauderdale, FL, Apr. 2016, paper JW3A.39.
- L. Zhu** and L. Najafizadeh, "Temporal Dynamics of fNIRS-Recorded Signals Revealed Via Visibility Graph," OSA Biomedical Optics Meeting, Fort Lauderdale, FL, Apr. 2016, Paper JW3A.53.
- T. Zeng, **L. Zhu**, Y. Wang and L. Najafizadeh, "On the Relationship Between Trial-to-Trial Response Time Variability and fNIRS-Based Functional Connectivity," OSA Biomedical Optics Meeting, Fort Lauderdale, FL, Apr. 2016, Paper JW3A.41.
- L. Zhu** and L. Najafizadeh, "Does Functional Connectivity Alter Across Similar Trials During Imaging Experiments?,"IEEE Signal Processing in Medicine and Biology Symposium (SPMB), Philadelphia, PA, Dec. 2014, pp. 1-4.
- L. Zhu**, M. Peifer and L. Najafizadeh "Towards Improving the Detection Power of Brain Imaging Experiments Using fNIRS,"OSA Technical Digest, Miami, FL, Apr. 2014, paper BM3A.29.
- M. Peifer, **L. Zhu** and L. Najafizadeh "Real-Time Classification of Actual vs Imagery Finger Tapping Using Functional Near-Infrared Spectroscopy,"OSA Technical Digest, Miami, FL, Apr. 2014, paper BM3A.34.
- Y. Huang, **L. Zhu**, C. Cheung, and L. Najafizadeh "A Low Temperature Coefficient Voltage Reference Utilizing BiCMOS Compensation Technique,"IEEE International Symposium on Circuits and Systems (ISCAS), Melbourne, Australia, 2014, pp. 922-925.
- Y. Huang, **L. Zhu**, C. Cheung and L. Najafizadeh "A Curvature-Compensation Technique Based on the Difference of Si and SiGe Junction Voltages for Bandgap Voltage Circuits,"IEEE International Symposium on Circuits and Systems (ISCAS), Melbourne, Australia 2014, pp. 914-917.



Under Review/Preparation

L. Zhu and L. Najafizadeh, "Averaging Strategies for fNIRS-Based Functional Brain Imaging Experiments," Under Preparation for Submission.

L. Zhu, A. Haddad, Y. Wang, L. Najafizadeh, "The Optimal Electrode/Optode Configuration in EEG-fNIRS Multi-Modal Functional Brain Imaging Experiments," Under Preparation for Submission.

Y. Huang, **L. Zhu**, F. Kong, C. Chun and L. Najafizadeh, "BiCMOS-Based Compensation: Towards Fully Temperature Corrected Bandgap Reference Circuits," Under Review.

L. Zhu and L. Najafizadeh, "Functional Brain Networks Analysis Via Multiplex Visibility Graph," Submitted to IEEE EMBC 2016.



Acknowledgement

- Dr. Laleh Najafizadeh (**Advisor**)
- Qualifying Examination Committee
 - Dr. Kristin Dana
 - Dr. Janne Lindqvist
 - Dr. Yanyong Zhang
 - Dr. Saman Zonouz
- Colleagues in the Integrated Systems and NeuroImaging Laboratory
 - Yi Huang, Tianjiao Zeng, Yunqi Wang, Ali Haddad, Maria Peifer
- Department of Electrical and Computer Engineering, Rutgers University
- Families and Friends



Reference

- [1] F. Amyot, T. Zimmermann, J. Riley, J. M. Kainerstorfer, V. Chernomordik, E. Mooshagian, L. Najafizadeh, F. Krueger, A. H. Gandjbakhche, and E. M. Wassermann, "Normative database of judgment of complexity task with functional near infrared spectroscopy - Application for TBI," *Neuroimage*, vol. 60, no. 2, pp. 879–883, 2012.
- [2] L. Zhu and L. Najafizadeh, "Temporal Dynamics of fNIRS-Recorded Signals Revealed Via Visibility Graph." Accepted for presentation at the 2016 OSA Biomedical Optics Meeting in Fort Lauderdale, Florida.
- [3] A. T. Buss, N. Fox, D. A. Boas, and J. P. Spencer, "Probing the early development of visual working memory capacity with functional near-infrared spectroscopy," *Neuroimage*, vol. 85, pp. 314–325, 2014.
- [4] R. C. Mesquita, M. A. Franceschini, and D. A. Boas, "Resting state functional connectivity of the whole head with near-infrared spectroscopy," *Biomedical optics express*, vol. 1, no. 1, pp. 324–336, 2010.
- [5] A. M. Chiarelli, G. L. Romani, and A. Merla, "Fast optical signals in the sensorimotor cortex: General linear convolution model applied to multiple source-detector distancebased data," *NeuroImage*, vol. 85, pp. 245–254, 2014.
- [6] K. Yanagisawa, H. Sawai, and H. Tsunashima, "Development of nirs-bci system using perceptron," in *12 th International Conference on Control, Automation and Systems (ICCAS)*. IEEE, 2012, pp. 1531–1535.
- [7] L. Zhu, M. Peifer, and L. Najafizadeh, "Towards improving the "detection" power of brain imaging experiments using fnirs," in *Biomedical Optics. Optical Society of America*, 2014, pp. BM3A–29.
- [8] L. Pollonini, C. Olds, H. Abaya, H. Bortfeld, M. S. Beauchamp, and J. S. Oghalai, "Auditory cortex activation to natural speech and simulated cochlear implant speech measured with functional near-infrared spectroscopy," *Hearing research*, vol. 309, pp. 84–93, 2014.
- [9] T. Wilcox, H. Bortfeld, R. Woods, E. Wruck, J. Armstrong, and D. Boas, "Hemodynamic changes in the infant cortex during the processing of featural and spatiotemporal information," *Neuropsychologia*, vol. 47, no. 3, pp. 657–662, 2009.
- [10] L. Zhu and L. Najafizadeh, "Does brain functional connectivity alter across similar trials during imaging experiments?" in *Signal Processing in Medicine and Biology Symposium (SPMB)*, 2014 IEEE. IEEE, 2014, pp. 1–4.
- [11] A. V. Medvedev, "Does the resting state connectivity have hemispheric asymmetry? A near-infrared spectroscopy study," *NeuroImage*, vol. 85, pp. 400–407, 2014.
- [12] G. Taga, H. Watanabe, and F. Homae, "Spatiotemporal properties of cortical haemodynamic response to auditory stimuli in sleeping infants revealed by multi-channel near-infrared spectroscopy," *Philosophical Transactions of the Royal Society A: Mathematical, Physical and Engineering Sciences*, vol. 369, no. 1955, pp. 4495–4511, 2011.
- [13] E. Başar, A. Gönder, C. Özesmi, and P. Uungan, "Dynamics of brain rhythmic and evoked potentials," *Biological Cybernetics*, vol. 20, no. 3-4, pp. 145–160, 1975.
- [14] D. H. Lange, H. T. Siegelmann, H. Pratt, and G. F. Inbar, "Overcoming selective ensemble averaging: unsupervised identification of event-related brain potentials," *Biomedical Engineering, IEEE Transactions on*, vol. 47, no. 6, pp. 822–826, 2000.
- [15] L. R. Bahl, F. Jelinek, and R. Mercer, "A maximum likelihood approach to continuous speech recognition," *IEEE Transactions on Pattern Analysis and Machine Intelligence*, no. 2, pp. 179–190, 1983.



Reference

- [16] Z. M. Kovács-Vajna, “A fingerprint verification system based on triangular matching and dynamic time warping,” *Pattern Analysis and Machine Intelligence, IEEE Transactions on*, vol. 22, no. 11, pp. 1266–1276, 2000.
- [17] E. J. Keogh and M. J. Pazzani, “Scaling up dynamic time warping for datamining applications,” in *Proceedings of the sixth ACM SIGKDD international conference on Knowledge discovery and data mining*. ACM, 2000, pp. 285–289.
- [18] J. Aach and G. M. Church, “Aligning gene expression time series with time warping algorithms,” *Bioinformatics*, vol. 17, no. 6, pp. 495–508, 2001.
- [19] A. Corradini, “Dynamic time warping for off-line recognition of a small gesture vocabulary,” in *Recognition, Analysis, and Tracking of Faces and Gestures in Real-Time Systems*, 2001. *Proceedings. IEEE ICCV Workshop on*. IEEE, 2001, pp. 82–89.
- [20] L. Gupta, D. L. Molfese, R. Tammana, and P. G. Simos, “Nonlinear alignment and averaging for estimating the evoked potential,” *Biomedical Engineering, IEEE Transactions on*, vol. 43, no. 4, pp. 348–356, 1996.
- [21] S. Herculano-Houzel, “The human brain in numbers: a linearly scaled-up primate brain,” *Frontiers in human neuroscience*, vol. 3, 2009.
- [22] M. Peifer, “Decoding brain states using functional brain imaging techniques,” Ph.D. dissertation, Rutgers University-Graduate School-New Brunswick, 2015.
- [23] W. Ou, “Spatio-temporal analysis in functional brain imaging,” Ph.D. dissertation, Massachusetts Institute of Technology, 2010.
- [24] B. He and Z. Liu, “Multimodal functional neuroimaging: integrating functional mri and eeg/meg,” *Biomedical Engineering, IEEE Reviews in*, vol. 1, pp. 23–40, 2008.
- [25] P. A. Jackson and D. O. Kennedy, “The application of near infrared spectroscopy in nutritional intervention studies,” 2013.
- [26] F. Scholkmann, S. Kleiser, A. J. Metz, R. Zimmermann, J. M. Pavia, U. Wolf, and M. Wolf, “A review on continuous wave functional near-infrared spectroscopy and imaging instrumentation and methodology,” *Neuroimage*, vol. 85, pp. 6–27, 2014.
- [27] L. Zhu, M. Peifer, and L. Najafizadeh, “Towards improving the“detection,”” in *Biomedical Optics. Optical Society of America*, 2014, pp. BM3A–29.
- [28] N. Naseer and K.-S. Hong, “fnirs-based brain-computer interfaces: a review,” *Frontiers in human neuroscience*, vol. 9, 2015.
- [29] M. Peifer, L. Zhu, and L. Najafizadeh, “Real-Time Classification of Actual vs Imagery Finger Tapping Using Functional Near-Infrared Spectroscopy,” in *Biomedical Optics. Optical Society of America*, 2014, pp. BM3A–34.
- [30] L. Kocsis, P. Herman, and A. Eke, “The modified Beer–Lambert law revisited,” *Physics in medicine and biology*, vol. 51, no. 5, p. N91, 2006.
- [31] L. Ji, J. Zhou, R. Zafar, S. Kantorovich, R. Jiang, P. R. Carney, and H. Jiang, “Cortical neurovascular coupling driven by stimulation of channelrhodopsin-2,” 2012.
- [32] S. Tak and J. C. Ye, “Statistical analysis of fnirs data: A comprehensive review,” *NeuroImage*, vol. 85, pp. 72–91, 2014.
- [33] H. Zhang, Y.-J. Zhang, C.-M. Lu, S.-Y. Ma, Y.-F. Zang, and C.-Z. Zhu, “Functional connectivity as revealed by independent component analysis of resting-state fnirs measurements,” *Neuroimage*, vol. 51, no. 3, pp. 1150–1161, 2010.
- [34] N. Karamzadeh, A. Medvedev, A. Azari, A. Gandjbakhche, and L. Najafizadeh, “Capturing dynamic patterns of task-based functional connectivity with eeg,” *NeuroImage*, vol. 66, pp. 311–317, 2013.
- [35] M. Hall, U. Chaudhary, G. Rey, and A. Godavarty, “Fronto-temporal mapping and connectivity using nirs for language-related paradigms,” *Journal of Neurolinguistics*, vol. 26, no. 1, pp. 178–194, 2013. *35th Annual International Conference of the IEEE. IEEE*, 2013, pp. 2160–2163.



Reference

- [36] P. P. Paul, H. Leung, D. A. Peterson, T. J. Sejnowski, and H. Poizner, "Detecting neural decision patterns using svm-based eeg classification," in Bioinformatics and Biomedical Engineering (iCBBE), 2010 4th International Conference on. IEEE, 2010, pp. 1–4.
- [37] C. Herff, D. Heger, F. Putze, J. Henrich, O. Fortmann, and T. Schultz, "Classification of mental tasks in the prefrontal cortex using fnirs," in Engineering in Medicine and Biology Society (EMBC), 2013 [38] P.-H. Chou and T.-H. Lan, "The role of near-infrared spectroscopy in alzheimer's disease," Journal of Clinical Gerontology and Geriatrics, vol. 4, no. 2, pp. 33–36, 2013.
- [39] J.-F. Démonet, G. Thierry, and D. Cardebat, "Renewal of the neurophysiology of language: functional neuroimaging," *Physiological reviews*, vol. 85, no. 1, pp. 49–95, 2005.
- [40] S. E. Petersen and J. W. Dubis, "The mixed block/event-related design," *Neuroimage*, vol. 62, no. 2, pp. 1177–1184, 2012.
- [41] M. Boecker, M. M. Buecheler, M. L. Schroeter, and S. Gauggel, "Prefrontal brain activation during stop-signal response inhibition: an event-related functional near-infrared spectroscopy study," *Behavioural brain research*, vol. 176, no. 2, pp. 259–266, 2007.
- [42] H. Watanabe, F. Homae, T. Nakano, and G. Taga, "Functional activation in diverse regions of the developing brain of human infants," *Neuroimage*, vol. 43, no. 2, pp. 346–357, 2008.
- [43] H. Sakoe and S. Chiba, "A dynamic programming approach to continuous speech recognition," in Proceedings of the seventh international congress on acoustics, vol. 3, 1971, pp. 65–69.
- [44] F. Petitjean, A. Ketterlin, and P. Gançarski, "A global averaging method for dynamic time warping, with applications to clustering," *Pattern Recognition*, vol. 44, no. 3, pp. 678–693, 2011.
- [45] T. Giorgino, "Computing and visualizing dynamic time warping alignments in r: the dtw package," *Journal of statistical Software*, vol. 31, no. 7, pp. 1–24, 2009.
- [46] A. M. Owen, K. M. McMillan, A. R. Laird, and E. Bullmore, "N-back working memory paradigm: A meta-analysis of normative functional neuroimaging studies," *Human brain mapping*, vol. 25, no. 1, pp. 46–59, 2005.
- [47] L. Wang, Y. Kuroiwa, T. Kamitani, T. Takahashi, Y. Suzuki, and O. Hasegawa, "Effect of interstimulus interval on visual p300 in parkinsonâZs disease," *Journal of Neurology, Neurosurgery & Psychiatry*, vol. 67, no. 4, pp. 497–503, 1999.
- [48] T. Ozawa, T. Aihara, Y. Fujiwara, Y. Otaka, I. Nambu, R. Osu, J. Izawa, and Y. Wada, "Detecting event-related motor activity using functional near-infrared spectroscopy," in 6th International IEEE/EMBS Conference on Neural Engineering (NER), 2013, pp. 1529–1532.
- [49] M. Xia, J. Wang, and Y. He, "Brainnet viewer: a network visualization tool for human brain connectomics," *PLoS One*, vol. 8, no. 7, p. e68910, 2013.
- [50] H. Watanabe, F. Homae, and G. Taga, "General to specific development of functional activation in the cerebral cortices of 2-to 3-month-old infants," *Neuroimage*, vol. 50, no. 4, pp. 1536–1544, 2010.
- [51] X. Cui, S. Bray, D. M. Bryant, G. H. Glover, and A. L. Reiss, "A quantitative comparison of nirs and fmri across multiple cognitive tasks," *Neuroimage*, vol. 54, no. 4, pp. 2808–2821, 2011.
- [52] Y. Zhang, D. H. Brooks, M. A. Franceschini, and D. A. Boas, "Eigenvector-based spatial filtering for reduction of physiological interference in diffuse optical imaging," *Journal of biomedical optics*, vol. 10, no. 1, pp. 011 014–01 101 411, 2005.
- [53] R. M. Birn, R. W. Cox, and P. A. Bandettini, "Detection versus estimation in event-related fmri: choosing the optimal stimulus timing," *Neuroimage*, vol. 15, no. 1, pp. 252–264, 2002.



Reference

- [54] E. Amaro and G. J. Barker, "Study design in fmri: basic principles," *Brain and cognition*, vol. 60, no. 3, pp. 220–232, 2006.
- [55] D. A. Soltysik, K. K. Peck, K. D. White, B. Crosson, and R. W. Briggs, "Comparison of hemodynamic response nonlinearity across primary cortical areas," *Neuroimage*, vol. 22, no. 3, pp. 1117–1127, 2004.
- [56] D. A. Handwerker, J. M. Ollinger, and M. D'Esposito, "Variation of bold hemodynamic responses across subjects and brain regions and their effects on statistical analyses," *Neuroimage*, vol. 21, no. 4, pp. 1639–1651, 2004.
- [57] V. Niennattrakul and C. A. Ratanamahatana, "Shape averaging under time warping," in *Electrical Engineering/Electronics, Computer, Telecommunications and Information Technology, 2009. ECTI-CON 2009. 6th International Conference on*, vol. 2. IEEE, 2009, pp. 626–629.
- [58] Zhang, Dandan, et al. "Enhanced response inhibition in experienced fencers." *Scientific reports* 5 (2015).
- [59] Herculano-Houzel, Suzana. "The human brain in numbers: a linearly scaled-up primate brain." *Frontiers in human neuroscience* 3 (2009): 31.
- [60] Thomas, David, et al., "The influence of unequal numbers of trials on comparisons of average event-related potentials." *Developmental neuropsychology*, 26(3): 735-774, 2004.
- [61] Cho, Hansang, et al. "Detection of neural activity in event-related fMRI using wavelets and dynamic time warping." *Optical Science and Technology, SPIE's 48th Annual Meeting*. International Society for Optics and Photonics, 2003.
- [62] Kirino, Eiji, et al. "Prefrontal activation evoked by infrequent target and novel stimuli in a visual target detection task: an event-related functional magnetic resonance imaging study." *The Journal of Neuroscience* 20.17 (2000): 6612-6618.



Thank you!